

1 **Observation of SOA tracers at a mountainous site in Hong Kong: chemical characteristics,**  
2 **origins and implication on particle growth**

3 X.P. Lyu <sup>1</sup>, H. Guo <sup>1\*</sup>, H.R. Cheng <sup>2\*\*</sup>, X.M. Wang <sup>3</sup>, X. Ding <sup>3</sup>, H.X. Lu <sup>1</sup>, D.W. Yao <sup>1</sup>, and C.  
4 Xu <sup>1</sup>

5 <sup>1</sup> Department of Civil and Environmental Engineering, The Hong Kong Polytechnic University,  
6 Hong Kong

7 <sup>2</sup> Department of Environmental Engineering, School of Resource and Environmental Sciences,  
8 Wuhan University, Wuhan, China

9 <sup>3</sup> State Key Laboratory of Organic Geochemistry, Guangzhou Institute of Geochemistry, Chinese  
10 Academy of Sciences, Guangzhou, China

11 Corresponding author: H. Guo ([ceguohai@polyu.edu.hk](mailto:ceguohai@polyu.edu.hk)); H.R. Cheng ([chenghr@whu.edu.cn](mailto:chenghr@whu.edu.cn))

12

13 **Abstract:** Secondary organic aerosol (SOA) is an important constituent of airborne fine particles.  
14 PM<sub>2.5</sub> (particles with aerodynamic diameters  $\leq 2.5 \mu\text{m}$ ) samples were collected at a mountainous  
15 site in Hong Kong in autumn of 2010, and analyzed for SOA tracers. Results indicated that the  
16 concentrations of isoprene SOA tracers ( $54.7 \pm 22.7 \text{ ng/m}^3$ ) and aromatics SOA tracers ( $2.1 \pm 1.6$   
17  $\text{ng/m}^3$ ) were on relatively high levels in Hong Kong. Secondary organic carbon (SOC) derived  
18 from isoprene, monoterpenes, sesquiterpenes and aromatics was estimated with the SOA tracer  
19 based approach, which constituted  $0.35 \pm 0.15 \mu\text{g/m}^3$  ( $40.6 \pm 5.7\%$ ),  $0.20 \pm 0.03 \mu\text{g/m}^3$  ( $30.4 \pm 5.5\%$ ),  
20  $0.05 \pm 0.02 \mu\text{g/m}^3$  ( $5.6 \pm 1.7\%$ ) and  $0.26 \pm 0.20 \mu\text{g/m}^3$  ( $21.3 \pm 8.2\%$ ) of the total estimated SOC.  
21 Biogenic SOC ( $0.60 \pm 0.18 \mu\text{g/m}^3$ ) dominated over anthropogenic SOC ( $0.26 \pm 0.20 \mu\text{g/m}^3$ ) at this  
22 site. In addition to the total estimated SOC ( $17.8 \pm 4.6\%$  of organic carbon (OC) in PM<sub>2.5</sub>),  
23 primary organic carbon (POC) emitted from biomass burning also accounted for a considerable  
24 proportion of OC ( $11.6 \pm 3.2\%$ ). Insight into the OC origins found that regional transport  
25 significantly ( $p < 0.05$ ) elevated SOC from  $0.37 \pm 0.17$  to  $1.04 \pm 0.39 \mu\text{g/m}^3$ . Besides, SOC load  
26 could also increase significantly if there was influence from local ship emission. Biomass  
27 burning related POC in regional air masses ( $0.81 \pm 0.24 \mu\text{g/m}^3$ ) was also higher ( $p < 0.05$ ) than that  
28 in samples affected by local air ( $0.29 \pm 0.35 \mu\text{g/m}^3$ ). Evidences indicated that SOA formation was  
29 closely related to new particle formation and the growth of nucleation mode particles, while  
30 biomass burning was responsible for some particle burst events in Hong Kong. This is the first  
31 SOA study in afforested areas of Hong Kong.

32 **Keywords:** Secondary organic aerosol, SOA tracer, biogenic SOA, regional transport, particle  
33 growth

## 34 **1. Introduction**

35 Atmospheric aerosol has been well recognized to affect global climate change (Stocker et al,  
36 2013), human health (Dockery et al., 1993; Pope III and Dockery, 2006), visibility (Appel et al.,  
37 1985) and sustainability of economy (Chameides et al., 1999). Secondary organic aerosol (SOA)  
38 has been identified to play critical roles in these effects (Maria et al., 2004; Volkamer et al., 2006;  
39 Baltensperger et al., 2008), thus receiving sufficient attentions in recent years.

40 So far, the scientific community has reached a consensus that volatile organic compounds (VOCs)  
41 from biogenic emissions and anthropogenic aromatics are key precursors of SOA (Forstner et al.,  
42 1997; Claeys, et al., 2004). In global scale, biogenic SOA is thought to be the greatest constituent  
43 of SOA, due to the worldwide largest emission of biogenic VOCs (*e.g.*, isoprene, monoterpenes  
44 and sesquiterpenes) and formation of biogenic SOA spanning a wide range of conditions (the  
45 level of NO<sub>x</sub>, humidity and aerosol acidity) (Kroll et al., 2006). However, anthropogenic SOA  
46 has also been found to be significant in urban areas (Volkamer et al., 2006). Furthermore, upon  
47 the findings that biogenic SOA correlates well with the indicators of anthropogenic emissions  
48 (Goldstein et al., 2009; Hoyle et al., 2011), it is believed that man-made air pollutants promote  
49 the formation of biogenic SOA, in addition to serving as SOA precursors themselves. These  
50 promoting effects at least include forming aerosol seeds, catalyzing photooxidation and  
51 transformation of biogenic VOCs and their oxidation products and changing the reaction  
52 pathways (*e.g.*, atmospheric fate of isoprene in low- and high-NO<sub>x</sub> environments) (Hoyle et al.,  
53 2011). It is believed that SOA is a collection of hundreds to thousands of organic chemicals  
54 featuring relatively low volatilities. To understand SOA formation and explore the potential  
55 sources, SOA speciation is of great necessity. However, due to the difficulty in chemical analysis  
56 of SOA tracers, the chemical compositions of SOA are far from being well understood. The  
57 traditional analysis by gas chromatography-mass spectrometer detector (GC-MSD) generally  
58 quantifies a total of less than 20 organic compounds in particles (Offenberg et al., 2007;  
59 Kleindienst et al., 2007). Although some advanced instruments have been developed nowadays,  
60 such as aerosol mass spectrometry and thermal desorption aerosol gas chromatography, they are  
61 either fragment-based or highly dependent upon the skills and knowledge of users (Williams et

62 al., 2014). Instead, SOA tracer based approach is a simplified method widely used to estimate the  
63 amount, precursors and sources of SOA (Kleindienst et al., 2007; Ding et al., 2012).

64 The SOA tracer based approach applies the laboratory obtained ratios between the sum of  
65 specific SOA tracers and total mass of SOA (or secondary organic carbon (SOC)) produced from  
66 individual (group of) species to the field measured SOA tracers (Kleindienst et al., 2007),  
67 roughly estimating SOA (SOC) derived from an individual VOC or VOC group. Table S1  
68 summarizes the VOC precursors, corresponding SOA tracers and the ratios between SOA tracers  
69 and SOA (or SOC), as reported by Kleindienst et al. (2007). The drawbacks of this method are  
70 obvious. For instance, it is controversial whether the laboratory obtained ratios can be directly  
71 applied to the field measured SOA tracers. However, it provides a feasible approach to estimate  
72 the SOA concentration, which is especially helpful in the cases of not well knowing the SOA  
73 compositions. More importantly, Offenberg et al. (2007) confirmed that the SOA tracer based  
74 approach was reliable through comparing with the results obtained from  $^{14}\text{C}$  contents.

75 Hong Kong, one of the most developed regions in East Asia, has a total territory area of  
76  $\sim 1.1 \times 10^3 \text{ km}^2$  and a total population of  $\sim 7$  million. Despite high population density, it keeps 24  
77 country parks and a vegetation coverage rate of 70%. Evergreen broadleaf trees are common in  
78 Hong Kong. Guenther et al. (2006) suggested that shrubs are large emitters of isoprene, a typical  
79 and most abundant biogenic VOC. The total emission amount of biogenic VOCs in Hong Kong  
80 is estimated as  $8.6 \times 10^3 \text{ ton C/a}$  (Tsui et al., 2009). Field measurements also revealed that  
81 isoprene in Hong Kong is relatively high (300-400 pptv) (Guo et al., 2007, 2012a). In contrast,  
82 aromatics are largely emitted from vehicular exhaust and solvent usage in Hong Kong. For  
83 example, toluene is one of the most abundant aromatics, with the level of 3-6 ppbv (Guo et al.,  
84 2004; Ho et al., 2004). Therefore, local emission of VOCs has a great potential forming SOA in  
85 Hong Kong. In addition to local SOA formation, regional transport is inevitable due to severe air  
86 pollution in upwind direction of Hong Kong (*i.e.*, inland Pearl River Delta (PRD) region).  
87 Studies confirmed that Hong Kong received SOA produced by isoprene and toluene from inland  
88 PRD region (Hu et al., 2008). However, the previous SOA studies in Hong Kong all focused on  
89 urban areas, which are not enough to understand the abundance, compositions and sources of  
90 SOA in low-altitude mountainous area where both anthropogenic and biogenic emissions are  
91 important.

92 In this study, SOC derived from isoprene, monoterpenes, sesquiterpenes and aromatics at a  
93 mountainous site in Hong Kong were estimated using a SOA tracer based approach. Local and  
94 regional contributions to SOC and biomass burning related POC were determined. Furthermore,  
95 in combination with particle size distribution simultaneously monitored by a scanning mobility  
96 particle sizer (SMPS), the relationships between SOA formation and particle growth were  
97 examined.

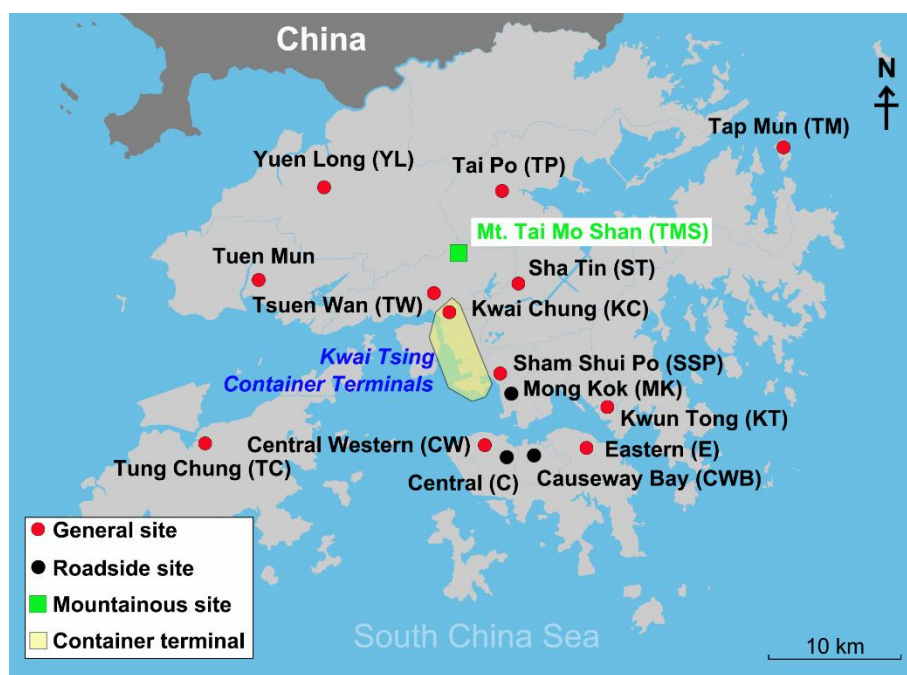
## 98 **2. Methodology**

### 99 **2.1 Sample collection**

100 Hong Kong, a coastal city surrounded by the South China Sea (SCS) to the east and south, is  
101 located in southern China. Under the dominance of subtropical monsoon climate, Hong Kong  
102 receives northerly winds originating from the heavily polluted PRD region in cool seasons  
103 (October-March), while prevailing southerly winds bring in clean air from SCS in warm seasons  
104 (April-August) (So and Wang, 2003). The sampling site (22.405° N, 114.118° E, 640 m a.s.l) was  
105 set up at the mountainside of the highest mountain in Hong Kong (Mt. Tai Mo Shan with the  
106 maximum altitude of 957 m, TMS). The vegetation on this mountain mainly includes *Acacia*  
107 *confusa*, *Lophotemon confertus*, *Machilus chekiangensis* and *Schima superba* below 550 m,  
108 while it turns to shrubs and grasses above 550 m (Guo et al., 2012b). As demonstrated in  
109 previous studies (Guo et al., 2013; Ling et al., 2014), regional transport of air pollutants from  
110 inland PRD, mesoscale circulation (mountain-valley breezes) and in situ atmospheric chemistry  
111 are the main processes that significantly influence air quality at this site. Figure 1 shows the  
112 geographical locations of the sampling site and air quality monitoring stations (AQMSs) of Hong  
113 Kong Environmental Protection Department (HKEPD).

114 From September 7 to November 26, 2010, a total of 19 PM<sub>2.5</sub> samples were collected. The  
115 instrument was an Anderson high volume PM<sub>2.5</sub> sampler, with a flow rate of 750 L/min. Pre-  
116 baked A4 size quartz fiber filters were used to collect the samples, which were stored in the  
117 refrigerator at -18 °C after sampling. Generally, each filter sampling lasted for 45-55 hours,  
118 except for the cases that the instrument stopped abnormally on some days due to thunderstorm-  
119 caused power outages. Table S2 lists the sample IDs, start and end dates & times. The origins of  
120 air masses, as distinguished by wind field and ratio of SO<sub>2</sub>/NO<sub>x</sub> (see section 3.3 for details), are  
121 also shown in the table. Additionally, the particle number concentrations and size distributions in  
122 the size range of 5.5-350.4 nm in 44 size bins were monitored by a scanning mobility particle

123 sizer (SMPS) from October 27 to November 29. Detailed introductions about the operation  
124 procedures of SMPS and data processing can be found in [Guo et al. \(2012a\)](#). We also collected  
125 ambient VOC samples during September 28-November 21. Inorganic trace gases ( $\text{SO}_2$ ,  $\text{CO}$ ,  $\text{NO}$ ,  
126  $\text{NO}_2$  and  $\text{O}_3$ ) and weather conditions were measured simultaneously with the  $\text{PM}_{2.5}$  sampling.  
127 Details about VOC sampling, VOC analysis and monitoring of trace gases are provided in [Guo et](#)  
128 [al. \(2013\)](#) and [Ling et al. \(2014\)](#).



129  
130 Figure 1 Geographic locations of the sampling site (TMS), AQMSs of HKEPD and the container  
131 terminal area where nine container terminals are located. Capital letters in the brackets are  
132 abbreviations of the site/stations

## 133 134 2.2 Chemical analysis

135 OC and element carbon (EC) in  $\text{PM}_{2.5}$  samples were analyzed using the thermo-optical  
136 transmittance method recommended by National Institute for Occupational Safety and Health  
137 (NIOSH) ([Birch, 1998](#)). The concentrations of OC and EC are shown in [Figure S1](#).

138 The method of SOA analysis was in line with that introduced by [Ding et al. \(2011\)](#). Briefly, the  
139 procedures for each sample include solvent extraction, derivation, analysis by GC-MSD, and  
140 identification and quantification of SOA tracers. 1/8 of each filter was extracted three times by  
141 sonication in the solvent of 40 mL of 1:1 (v/v) dichloride methane (DCM)/methanol mixture.  
142 Prior to extraction, the internal standards (hexadecanoic acid- $\text{D}_{31}$ , phthalic acid- $\text{D}_4$  and

143 levoglucosan-<sup>13</sup>C<sub>6</sub>) were spiked into the samples. The three-time extracts of each sample were  
144 combined, filtered and concentrated to ~2 mL, which was further divided into two parts for  
145 methylation and silylation derivation, respectively. In methylation derivation, the extract  
146 experienced a gentle nitrogen blow to dryness, and subsequent addition of 200 μL of DCM, 10  
147 μL of methanol and 300 μL of freshly prepared diazomethane. Then, it was kept in room  
148 temperature for one hour to derivatize acids to methyl esters, after which the sample was blown  
149 to 200 μL and used for analysis of some α-pinene SOA tracers (Pinonic acid, pinic acid and 3-  
150 methyl-1,2,3-butanetricarboxylic acid). The silylation reagent was 100 μL of pyridine and 200  
151 μL of N,O-bis-(trimethylsilyl)-trifluoroacetamide (BSTFA) plus 1% trimethylchlorosilane  
152 (TMCS). Differently, the derivation was carried out in an oven at 70 °C for one hour. One α-  
153 pinene SOA tracer (3-hydroxyglutanic acid) and tracers for isoprene SOA, sesquiterpenes SOA,  
154 and toluene SOA were analyzed from the silylated sample. An Agilent 5973N GC/MSD was  
155 employed to do the analysis. The identification of SOA tracers was based on the comparison of  
156 mass spectra with previous studies, and their retention time in GC chromatogram with other  
157 known compounds as the references. Pinonic acid and pinic acid were quantified by authentic  
158 standards. However, due to lack of standards, other α-pinene SOA tracers, isoprene SOA tracers,  
159 β-Caryophyllenic acid and 2,3-dihydroxy-4-oxopentanoic acid were quantified using pinic acid  
160 (PA), erythritol, octadecanoic acid and azelaic acid, respectively. The detection limits (DLs) for  
161 pinonic acid, pinic acid, erythritol, octadecanoic acid and azelaic acid were 0.05, 0.07, 0.06, 0.09,  
162 and 0.11 ng/m<sup>3</sup>, respectively. Levoglucosan was also quantified with the DL of 0.15 ng/m<sup>3</sup>. The  
163 SOA tracers analyzed in this study are highlighted in [Table S1](#).

### 164 **2.3 Quality assurance and quality control**

165 In this study, internal standards were not spiked on the filters before sampling, to avoid their  
166 influences on OC analysis. According to the saturation concentrations of SOA tracers calculated  
167 by [Ding et al. \(2016\)](#), SOA tracers analyzed in this study were of low volatilities, except for  
168 pinonic acid. Therefore, pinonic acid in airborne PM<sub>2.5</sub> might be underestimated due to the blow-  
169 off effect during sampling, which however should not be significant to other SOA tracers.  
170 Recovery target compounds were spiked in the samples before analysis of SOA tracers. The  
171 recovery rates were 104±2%, 68±13%, 62±14%, 78±10%, 81±9% and 87±4% for pinonic acid,  
172 pinic acid, erythritol, octadecanoic acid, azelaic acid and levoglucosan, respectively. Since



173 internal standards were added into the samples prior to analysis, we did not use the recovery  
174 rates to correct the concentrations of SOA tracers.

## 175 **2.4 Processing of SMPS data**

176 In this study, particles measured by SMPS were divided into nucleation (5.5-24.7 nm), Aitken  
177 (24.7-101.4 nm) and accumulation modes (101.4-350.4 nm). Geometric mean diameter (GMD)  
178 for nucleation mode particles (5.5-24.7 nm) was calculated using the following equations (Guo et  
179 al., 2012a).

$$180 \text{GRs} = \frac{d_{GMD}}{d_t} \quad (\text{Equation (1)})$$

$$181 \text{GMD} = e^{(\sum n_i \ln d_i)/N} \quad (\text{Equation (2)})$$

$$182 \frac{d_N}{d_{\log D_p}} = \frac{\Delta N}{\log D_p^2 - \log D_p^1} \quad (\text{Equation (3)})$$

183 where  $n_i$  is the particle number concentration in the  $i^{\text{th}}$  bin with upper diameter of  $d_i$ ,  $N$  represents  
184 the total number concentration ( $\text{cm}^{-3}$ ).  $\Delta N$  is the particle number concentration in the size bin  
185 with upper and lower limit diameter of  $D_p^2$  and  $D_p^1$ , respectively.

186 Condensation sink (CS), which describes the loss rate of vapor molecules and newly formed  
187 particles on the pre-existing aerosol particles, was calculated as follows (Kulmala et al., 2005):

$$188 \text{CS} = 2\pi D \int D_p \beta_m(D_p) n(D_p) dD_p = 2\pi D \sum_i \beta_{mi} D_{pi} N_i \quad (\text{Equation (4)})$$

189 where  $D$  is the diffusion coefficient of the condensing vapor,  $\beta_m$  is the transitional regime  
190 correction factor,  $D_p$  denotes the particle diameter,  $n$  and  $N$  represent the particle numbers.  $\beta_{mi}$ ,  
191  $D_{pi}$  and  $N_i$  are the specific values for a given size bin ( $i$ ). Growth factor calculated according to  
192 Laakso et al. (2004) was used to calibrate the dry particle size measured by SMPS.

193

## 194 **3. Results and discussion**

### 195 **3.1 Concentrations of SOA tracers**

196 Table 1 shows the average concentrations of SOA tracers derived from different precursors at  
197 TMS. Isoprene SOA tracers were the most abundant ( $54.7 \pm 22.7 \text{ ng/m}^3$ ), followed by the tracers  
198 generated from monoterpenes ( $26.3 \pm 4.5 \text{ ng/m}^3$ ), aromatics ( $2.1 \pm 1.6 \text{ ng/m}^3$ ) and sesquiterpenes  
199 ( $1.1 \pm 0.4 \text{ ng/m}^3$ ). Figure 2 compares the concentrations of SOA tracers between previous studies  
200 and the present study. The number and species of SOA tracers for the same precursor were the  
201 same. For the cases that total concentration of monoterpenes SOA tracers was given (e.g.,  
202 Offenberg et al., 2011), a factor was applied to the total concentration to roughly estimate the

203 sum of monoterpenes SOA tracers with the number and species identical to this study (see  
204 section S1 and [Figure S2 in the Supplement](#)). It was found that isoprene SOA tracers at TMS  
205 were on relatively high level ( $54.7 \pm 22.7 \text{ ng/m}^3$ ), comparable to or even higher than those  
206 detected in the forest ( $61.4 \pm 30.4 \text{ ng/m}^3$  in [Kleindienst et al. \(2007\)](#) and  $39.0 \pm 17.2 \text{ ng/m}^3$  in  
207 [Offenberg et al. \(2011\)](#)). In fact, isoprene at TMS was relatively low (2-517 pptv), the high  
208 isoprene SOA tracers indicated that biogenic SOA formation at this site might be enhanced by  
209 anthropogenic emissions, *e.g.*, sufficient aerosol seeds from SO<sub>2</sub>-related new particle formation  
210 ([Guo et al., 2012a](#)). Certainly, regional transport could also contribute to high isoprene SOA  
211 tracers, as reported by [Hu et al. \(2008\)](#). For the anthropogenic SOA, the tracer produced by  
212 aromatics (2,3-dihydroxy-4-oxopentanoic acid) was noticeable. Although the average 2,3-  
213 dihydroxy-4-oxopentanoic acid in this study ( $2.1 \pm 1.6 \text{ ng/m}^3$ ) was not significantly higher than  
214 that in other studies ( $p > 0.05$ ), its maximum value reached  $13.5 \text{ ng/m}^3$ . Given abundant aromatics  
215 in the atmosphere of Hong Kong and mesoscale circulations between TMS and the surrounding  
216 urban areas, local formation could be an important factor contributing to high aromatics SOA at  
217 TMS. Moreover, it was reported that 2,3-dihydroxy-4-oxopentanoic acid at an urban  
218 background site in inland PRD was very high ( $13.1 \text{ ng/m}^3$ ) ([Ding et al., 2012](#)). Hence, regional  
219 transport might be partially responsible for the relatively high aromatics SOA tracer in Hong  
220 Kong. SOA tracers derived from monoterpenes and sesquiterpenes were on moderate levels,  
221 compared to other studies.

222 3-Methyl-1,2,3-butanetricarboxylic acid and 3-hydroxyglutanic acid, formed from monoterpenes  
223 oxidation in the presence of NO<sub>x</sub> ([Claeys et al., 2007](#); [Eddingsaas et al., 2012](#)), dominated the  
224 measured monoterpenes SOA tracers, consistent with those at an urban background site in inland  
225 PRD ([Ding et al., 2012](#)). Pinonic acid and pinic acid, formed from OH oxidation of  $\alpha$ -pinene in  
226 NO<sub>x</sub> free environment or ozonolysis of  $\alpha$ -pinene ([Eddingsaas et al., 2012](#)), were also higher than  
227 those in urban areas of Hong Kong (almost below DLs) ([Hu et al., 2008](#)). Since NO<sub>x</sub> was at the  
228 magnitude of several ppbv, the higher pinonic acid and pinic acid were likely due to the higher  
229 O<sub>3</sub> ( $69.2 \pm 2.4 \text{ ppbv}$  at TMS and  $30.8 \pm 2.6 \text{ ppbv}$  at the mountain foot) at this mountainous site. In  
230 addition, other tracers including 3-hydroxy-4,4-dimethylglutaric acid, 3-isopropylpentanedioic  
231 acid, 3-acetylpentanedioic acid and 3-acetylhexanedioic acid, which were not measured in this  
232 study, accounted for  $46.9 \pm 4.0\%$  of the total amount of tracers according to [Kleindienst et al.](#)  
233 ([2007](#)). Of the isoprene SOA tracers, 2-methylthreitol and 2-methylerythritol are representative

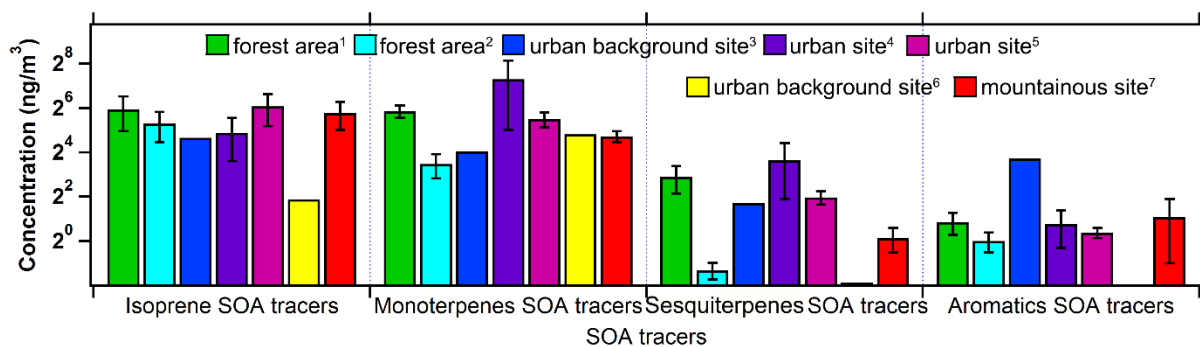


234 products formed through the photooxidation of isoprene hydroxyhydroperoxides and acid  
 235 catalysis of epoxydiols of isoprene in low NO<sub>x</sub> environment when RO<sub>2</sub> reacting with HO<sub>2</sub>  
 236 dominated the loss of RO<sub>2</sub> (Claeys et al., 2004; Surratt et al., 2010). In this study, they accounted  
 237 for 83.5±8.1% of the total isoprene tracers. However, NO<sub>x</sub> was not low enough and RO<sub>2</sub> reacting  
 238 with NO was the main sink of RO<sub>2</sub> (Ling et al., 2014), implying that other mechanisms might  
 239 enhance the formation of 2-methyltetrols (sum of 2-methylthreitol and 2-methylerythritol) at this  
 240 site, such as acid catalysis (Surratt et al., 2007).

241 Table 1 Average concentrations of SOA tracers derived from monoterpenes, isoprene,  
 242 sesquiterpenes and aromatics (mean±95% confidence interval (C.I.)).

VOC precursor	SOA tracer	Concentration (ng/m <sup>3</sup> )
Monoterpenes	Pinonic acid	1.2±0.4
	Pinic acid	2.0±0.6
	3-methyl-1,2,3-butanetricarboxylic acid	16.0±3.5
	3-hydroxyglutanic acid	7.1±2.7
	Sum 1	26.3±4.5
Isoprene	2-Methylthreitol	14.7±6.6
	2-Methylerythritol	31.2±13.1
	2-methylglyceric acid	5.2±3.1
	cis-2-Methyl-1,3,4-trihydroxy-1-butene	0.8±0.5
	trans-2-Methyl-1,3,4-trihydroxy-1-butene	2.0±1.3
	3-Methyl-2,3,4-trihydroxy-1-butene	0.7±0.3
	Sum 2	54.7±22.7
Sesquiterpenes	β-Caryophyllenic acid	1.1±0.4
Aromatics	2,3-Dihydroxy-4-oxopentanoic acid	2.1±1.6

243



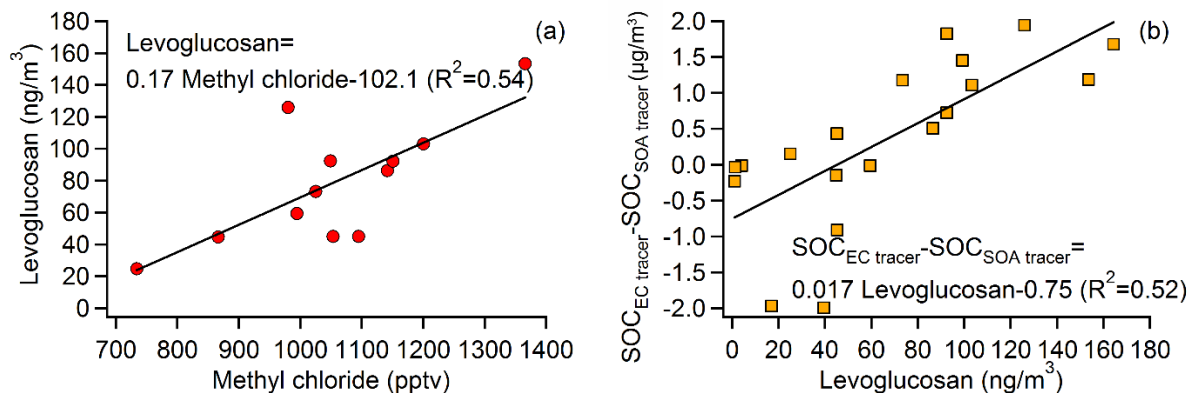
244  
 245 Figure 2 Comparison of SOA tracers between previous studies and this study. <sup>1</sup>Kleindienst et al.  
 246 (2007); <sup>2</sup>Offenberg et al. (2011); <sup>3</sup>Ding et al. (2012); <sup>4</sup>Hu et al. (2008); <sup>5</sup>Lewandowski et al.  
 247 (2008); <sup>6</sup>Haddad et al. (2011); <sup>7</sup>this study.

248  
 249 **3.2 Estimate of SOC**

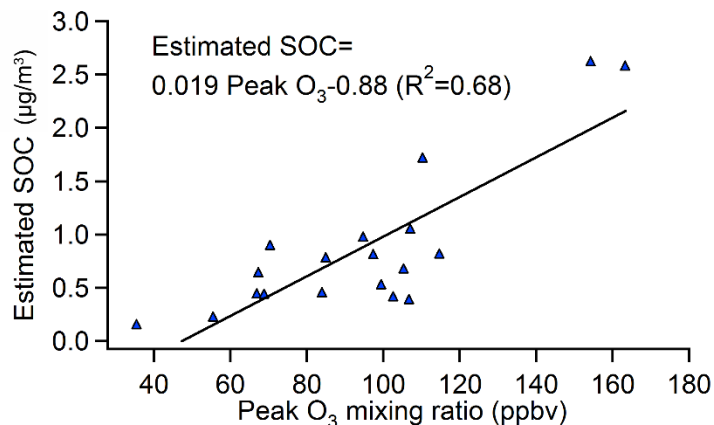
250 Both the EC tracer method and SOA tracer method were used to estimate SOC (details about  
 251 both methods are provided in section S2 of the Supplement). To apply the SOA tracer method,  
 252 the sum of monoterpenes SOA tracers was scaled by a factor of 1.79 (see section S1 and [Figure](#)  
 253 [S2](#) for details). [Figure S3](#) compares the SOC estimated by these two methods. SOC estimated by  
 254 EC tracer method ( $SOC_{EC\ tracer}$ ) were generally higher ( $p < 0.01$ ) than those estimated by SOA  
 255 tracer method ( $SOC_{SOA\ tracer}$ ), except for samples TMS1, TMS3 and TMS8. [Ding et al. \(2012\)](#)  
 256 indicated that the EC tracer method might overestimate SOC, because it blended some primary  
 257 OC (POC) from biomass burning with SOC. This inference was supported by the good  
 258 correlation between the difference of SOC estimated by these two methods ( $SOC_{EC\ tracer} - SOC_{SOA}$   
 259  $_{tracer}$ ) and levoglucosan, a tracer of biomass burning.

260 In addition to levoglucosan, methyl chloride ( $CH_3Cl$ ) is an indicator of biomass burning  
 261 ([Rudolph et al., 1995](#)). [Figure 3](#) plots the correlation between levoglucosan and  $CH_3Cl$  at TMS,  
 262 as well as that between  $SOC_{EC\ tracer} - SOC_{SOA\ tracer}$  and levoglucosan. As expected, levoglucosan  
 263 fairly correlated with  $CH_3Cl$  ( $R^2 = 0.54$ ), further confirming the reliability of levoglucosan as the  
 264 tracer of biomass burning. Consistent with [Ding et al. \(2012\)](#), good correlation was found  
 265 between  $SOC_{EC\ tracer} - SOC_{SOA\ tracer}$  and levoglucosan ( $R^2 = 0.52$ ). This verified that the EC tracer  
 266 method overestimated SOC due to the interference of biomass burning. Exceptionally,  $SOC_{EC}$   
 267  $_{tracer}$  was remarkably lower than  $SOC_{SOA\ tracer}$  for the samples TMS1, TMS3 and TMS8 ( $p < 0.05$ ).  
 268 Further investigation found that on the sampling days of TMS1 and TMS3, the daily maximum  
 269 hourly  $O_3$  mixing ratio, referred to as peak  $O_3$ , was extremely high, with the values being the

270 second (154.4 ppbv) and first (163.4 ppbv) highest among the 19 filter samples, respectively,  
 271 while during the sampling period of TMS8, the peak O<sub>3</sub> also reached 94.8 ppbv. In contrast, the  
 272 average of peak O<sub>3</sub> values on the sampling days of other PM<sub>2.5</sub> filter samples was only 77.6 ppbv.  
 273 Since high O<sub>3</sub> levels generally imply strong photochemical reactivity, high productions of SOA  
 274 are also expected on these days. Hence, the higher SOC<sub>SOA tracer</sub> values observed in TMS1, TMS3  
 275 and TMS8 were understandable. We also found that there was no correlation between SOC<sub>EC</sub>  
 276 tracer and peak O<sub>3</sub> (not shown), whereas SOC<sub>SOA tracer</sub> correlated well with peak O<sub>3</sub> (R<sup>2</sup>=0.68), as  
 277 shown in Figure 4, implying that the formation of secondary products, *i.e.*, SOA and O<sub>3</sub>, depends  
 278 upon the oxidative capacity of the atmosphere and they may also influence each other. Therefore,  
 279 the SOA tracer method was believed to be more reliable and thus adopted in this study. Hereafter,  
 280 SOC refers to SOC<sub>SOA tracer</sub>, unless otherwise specified.



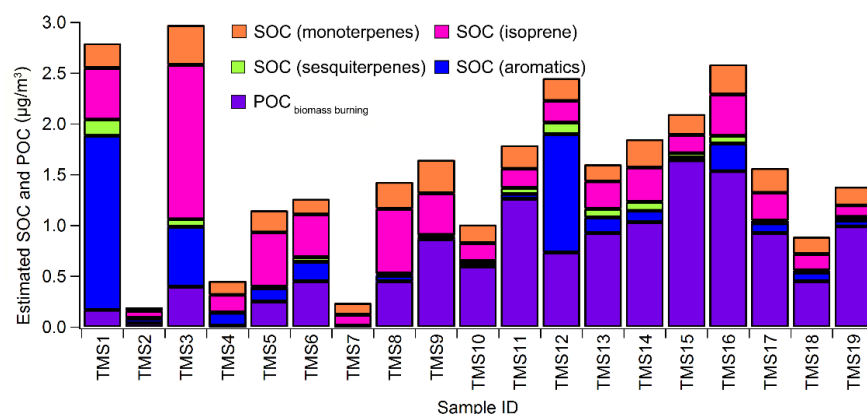
281  
 282 Figure 3 Linear correlations between (a) levoglucosan and CH<sub>3</sub>Cl, and (b) SOC<sub>EC tracer</sub> - SOC<sub>SOA</sub>  
 283 tracer and levoglucosan.



284  
 285 Figure 4 Linear correlation between SOC<sub>SOA tracer</sub> and peak O<sub>3</sub>.

286

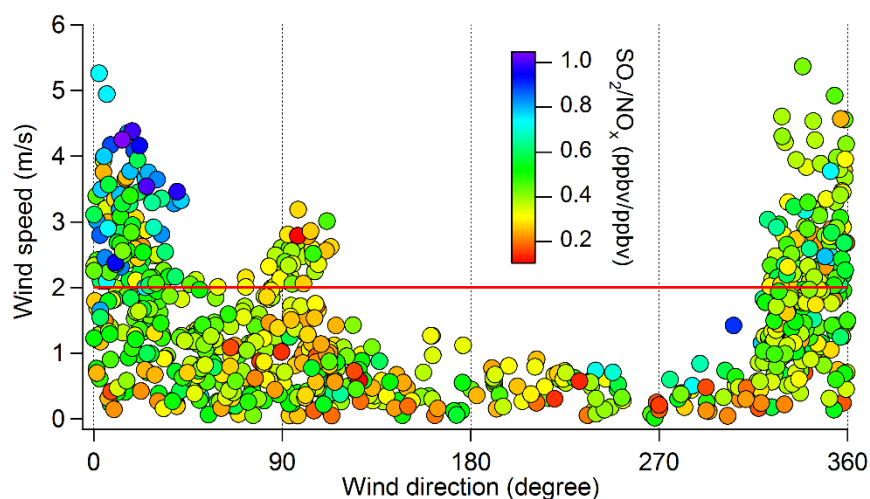
287 Figure 5 shows SOC produced by different groups of VOCs estimated using the SOA tracer  
 288 based approach, and biomass burning related POC ( $\text{POC}_{\text{biomass burning}}$ ).  $\text{POC}_{\text{biomass burning}}$  was  
 289 estimated by  $0.01 (\mu\text{g}/\text{ng}) \times \text{levoglucosan} (\text{ng}/\text{m}^3)$  (Lee et al., 2008). On average, SOC and  $\text{POC}_{\text{biomass burning}}$   
 290 constituted  $0.86 \pm 0.31 \mu\text{g}/\text{m}^3$  ( $17.8 \pm 4.6\%$ ) and  $0.67 \pm 0.22 \mu\text{g}/\text{m}^3$  ( $11.6 \pm 3.2\%$ ) of OC  
 291 (provided in Figure S1), respectively. The rest of OC were undetermined due to unknown  
 292 sources and precursors of OC. The total SOC comprised anthropogenic (*i.e.*, aromatics) and  
 293 biogenic (*i.e.*, isoprene, monoterpenes and sesquiterpenes) SOC, with the fractions of  $21.3 \pm 8.2\%$   
 294 ( $0.26 \pm 0.20 \mu\text{g}/\text{m}^3$ ) and  $78.7 \pm 8.2\%$  ( $0.60 \pm 0.18 \mu\text{g}/\text{m}^3$ ), respectively. Although anthropogenic  
 295 SOC (ASOC) was significantly lower than biogenic SOC (BSOC) ( $p < 0.05$ ), ASOC had its  
 296 highest value of  $1.71 \mu\text{g}/\text{m}^3$  in the sample TMS1, and BSOC reached its maximum in sample  
 297 TMS3 ( $2.03 \mu\text{g}/\text{m}^3$ ). As mentioned earlier, the two samples were collected on the days with very  
 298 high  $\text{O}_3$ , indicating that aromatics and biogenic VOCs might be responsible for the high SOC in  
 299 TMS1 and TMS3, respectively. However, VOC samples were not simultaneously collected  
 300 during the collection of these two samples. Instead, the sample TMS12 was a good example  
 301 because ASOC was the second highest ( $1.2 \mu\text{g}/\text{m}^3$ ), and the daily average mixing ratio of toluene  
 302 coincidentally reached 4.0 ppbv during the TMS12 sampling period, the highest value among all  
 303 VOC samples, which further confirmed the reliability of SOA tracer method in estimating SOC.  
 304 Among SOC derived from biogenic VOCs, isoprene made the highest contribution ( $54.2 \pm 5.3\%$   
 305 of BSOC and  $42.7 \pm 5.9\%$  of total SOC), followed by monoterpenes ( $37.9 \pm 4.6\%$  and  $30.4 \pm 5.5\%$ ,  
 306 respectively) and sesquiterpenes ( $7.9 \pm 2.7\%$  and  $5.6 \pm 1.7\%$ , respectively).



307  
 308 Figure 5 Concentrations of estimated SOC derived from monoterpenes, isoprene, sesquiterpenes  
 309 and aromatics and  $\text{POC}_{\text{biomass burning}}$ .

### 310 3.3 Local and regional contributions to SOC

311 In line with the method used in Guo et al. (2013), the local and regional air masses were  
 312 distinguished with the wind direction (WD) and wind speed (WS) monitored at TMS. Briefly,  
 313 the northerly winds ( $0^\circ < \text{WD} < 90^\circ$  or  $270^\circ < \text{WD} < 360^\circ$ ) with WS higher than 2 m/s were considered  
 314 to be capable of delivering air pollutants from the heavily polluted inland PRD region to the site.  
 315 In these cases, the air masses were believed to be subject to regional influences. Otherwise, the  
 316 site was dominated by local air. To validate this method, Figure 6 shows the hourly ratios of  
 317  $\text{SO}_2/\text{NO}_x$  for the air masses in different wind directions/speeds. Overall, the  $\text{SO}_2/\text{NO}_x$  ratios were  
 318 higher for regional air masses, particularly when  $0^\circ < \text{WD} < 90^\circ$  and  $\text{WS} > 2$  m/s. This coincided  
 319 with the lower sulfur content in vehicle fuels and higher vehicle emissions of  $\text{NO}_x$  in Hong Kong  
 320 (Wang and So, 2003; Guo et al., 2009). For the 24-48 hr  $\text{PM}_{2.5}$  samples (*i.e.*, duration of 1-2  
 321 days), the regional influence was not unexpected given that the northerly wind was stronger than  
 322 2 m/s for at least one hour on each sampling day. It was noteworthy that during the sampling  
 323 periods of TMS1 and TMS16 (influenced by regional air),  $\text{SO}_2$  was exclusively high at the  
 324 HKEPD AQMSs in vicinity of the ship container terminals, *e.g.*, KC, SSP and TW (see Figure 1).  
 325 Figure S4 presents  $\text{SO}_2$  distributions at 14 AQMSs in Hong Kong during these two periods. In  
 326 view of the fact that ship is a significant emitter of  $\text{SO}_2$ , the influence of local ship emission was  
 327 also suspected for the two samples. According to these inferences, Table S2 lists the categories  
 328 of the samples affected by regional air, local air, and local ship emissions, respectively.



329  
 330 Figure 6 Hourly ratios of  $\text{SO}_2/\text{NO}_x$  for the air masses in different wind directions/speeds at TMS.  
 331 Table 2 summarizes the concentrations of SOC and  $\text{POC}_{\text{biomass burning}}$  in different categories of air  
 332 masses. Note that since the samples TMS1 and TMS16 were influenced by both regional air and  
 333 local ship emission, they were separately discussed later. It was found that SOC derived from

334 individual group/species and total SOC in regional air were all significantly ( $p<0.05$ ) higher than  
 335 that in local air, suggesting that SOC at TMS was elevated by regional transport. Despite  
 336 possible influences of local ship emissions in TMS1 and TMS16, the concentrations of SOC and  
 337 POC in these two samples were well within the ranges of those in regional air, except for  
 338 aromatics SOC ( $1.71 \mu\text{g}/\text{m}^3$ ) in sample TMS1. The extremely high aromatics SOC in TMS1  
 339 might be caused by ship emissions which could be laden with high concentrations of aromatics.  
 340 Contradictorily, SOC derived from aromatics was remarkably lower in TMS16 ( $0.27 \mu\text{g}/\text{m}^3$ ).  
 341 This discrepancy might be explained by the differences of fuel types and operating conditions of  
 342 the ship engines, which were repeatedly proved to affect the emission characteristics of ship  
 343 engines (Reda et al., 2014; Sippula et al., 2014). Similar to SOC, POC also showed a  
 344 significantly higher level in regional air ( $0.81\pm 0.24 \mu\text{g}/\text{m}^3$ ) than that in local air ( $0.29\pm 0.35$   
 345  $\mu\text{g}/\text{m}^3$ ) ( $p<0.05$ ). Since the high concentration of  $\text{POC}_{\text{biomass burning}}$  in regional air was partially  
 346 contributed by TMS16 ( $\text{POC}_{\text{biomass burning}} = 1.54 \mu\text{g}/\text{m}^3$ ), a sample jointly influenced by regional  
 347 air and local ship emission, specific insight was given to this sample. Firstly, ship emission was  
 348 not likely to be the culprit of high  $\text{POC}_{\text{biomass burning}}$ , as no study reported ship emission of  
 349 levoglucosan, the biomass burning tracer used to calculate  $\text{POC}_{\text{biomass burning}}$  in this study. Instead,  
 350 we found that another sample under the influence of regional air (TMS15) had comparable  $\text{POC}_{\text{biomass burning}}$   
 351 ( $1.64 \mu\text{g}/\text{m}^3$ ). Furthermore,  $\text{CH}_3\text{Cl}$ , another tracer of biomass burning, increased  
 352 noticeably under northerly winds in sample TMS16, indicating the regional transport of biomass  
 353 burning plumes into Hong Kong. In fact, nearly no fire spot in local Hong Kong was observed by  
 354 the satellite during the sampling, compared to some open fires detected in upwind directions (see  
 355 [Figure S5](#)). Therefore,  $\text{POC}_{\text{biomass burning}}$  in TMS16 was reasonably speculated to be elevated by  
 356 regional biomass burning plumes. Upon this inference, we concluded that regional transport  
 357 significantly contributed to  $\text{PM}_{2.5}$ -bounded POC in Hong Kong.

358

359 Table 2 Mean $\pm$ 95% C.I. of SOC and POC in different categories of air masses (Unit:  $\mu\text{g}/\text{m}^3$ ).

	Local air	Regional air	TMS1 <sup>*</sup>	TMS16 <sup>*</sup>
SOC (monoterpenes)	0.13 $\pm$ 0.06	0.23 $\pm$ 0.03	0.23	0.28
SOC (isoprene)	0.16 $\pm$ 0.07	0.42 $\pm$ 0.18	0.51	0.41
SOC (sesquiterpenes)	0.01 $\pm$ 0.01	0.06 $\pm$ 0.02	0.16	0.07
SOC (aromatics)	0.07 $\pm$ 0.04	0.33 $\pm$ 0.26	1.71	0.27



POC <sub>biomass burning</sub>	0.29±0.35	0.81±0.24	0.17	1.54
Total SOC	0.37±0.17	1.04±0.39	2.61	1.04

360 \* 95% C.I. is not available for a single sample.

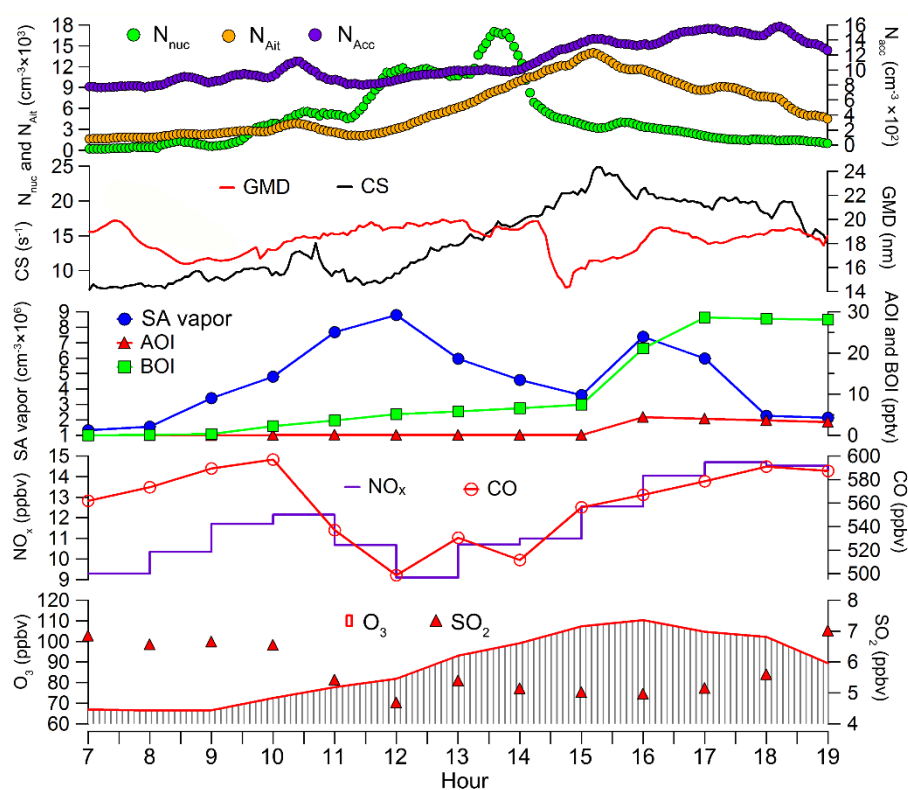
### 361 **3.4 Implications to particle formation and growth**

362 As an important constituent of airborne particles, SOA plays critical role in particle formation  
 363 and growth (Jang et al., 2003). The relationships between SOA formation and particle  
 364 formation/growth were investigated on three selected days (October 31, November 09 and  
 365 November 19) when SOC were among the highest of all the samples and SMPS data were  
 366 available. Figures 7-9 show the evolutions of particle numbers, GMD of nucleation mode  
 367 particles, CS, the simulated sulfuric acid (SA) vapor, oxidized intermediates of aromatics (AOI),  
 368 oxidized intermediates of biogenic VOCs (BOI), and the measured inorganic trace gases. Details  
 369 about the modelling of SA vapor, AOI and BOI are provided in Section S3 and Table S3 in the  
 370 Supplement. For convenience of analysis, the hourly mixing ratios of biogenic VOCs (BVOCs),  
 371 aromatics and CH<sub>3</sub>Cl are presented in Figure S6.

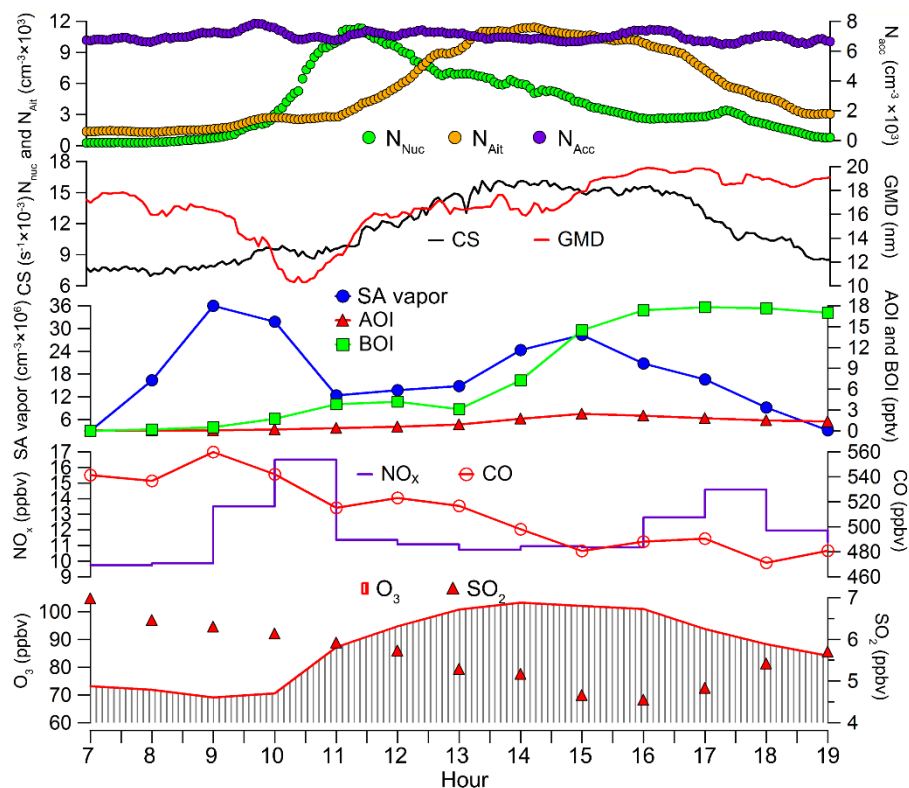
372 In Figures 7-8, the number concentration of nucleation mode particles ( $N_{nuc}$ ) increased  
 373 substantially in the morning of October 31 (11:00-12:00) and November 09 (10:00-11:00),  
 374 followed by the increases of number of Aitken mode particles ( $N_{Ait}$ ). Prior to the increases of  
 375  $N_{nuc}$ , the simulated SA vapor began to increase about 3 hours earlier. These were consistent with  
 376 the findings in Guo et al. (2012a) who reported that the increase of  $N_{nuc}$  was caused by new  
 377 particle formation (NPF) events occurred on both days, and SA vapor played important roles in  
 378 NPF. However, we further found that the oxidation intermediates of BVOCs (*i.e.*, BOI) also  
 379 increased slightly ahead of the rise of  $N_{nuc}$ , which might suggest that the oxidation of BVOCs  
 380 also made some contributions to NPF. In fact, the involvement of BVOCs in NPF at this  
 381 afforested site has been speculated by Guo et al. (2012a), which is confirmed with the aid of  
 382 model simulations in this study.

383 Moreover, we noticed that the nucleation mode particles experienced obvious growth with the  
 384 rate of 1.9 nm/h (15:00-16:00) and 1.4 nm/h (14:00-16:00) in the afternoon of October 31 and  
 385 November 09, respectively. Both growths occurred under the conditions of high  $N_{Ait}$  and high  
 386 CS, differing from NPF events. Meanwhile, O<sub>3</sub> was on high level, which meant strong oxidative  
 387 capacity of the atmosphere. Correspondingly, the simulated SA vapor, AOI and BOI showed  
 388 great increments simultaneously with or 1-2 hours earlier than the increase of GMD. It is

389 noteworthy that the significant increases of AOI and BOI were also attributable to the rapid  
 390 increases of VOCs (see Figure S6), in addition to strong atmospheric oxidative capacity. This  
 391 suggested that the photo-oxidation of VOCs also facilitated the growth of nucleation mode  
 392 particles. The prompt responses of particle growth to the increments of oxidation products on  
 393 October 31 (rather than 1.5 hours' delay on November 09) were likely caused by the much more  
 394 abundant BOI (~22.7 pptv) than that on November 09 (~13.5 pptv). Besides, the lower initial  
 395 GMD before its increase on October 31 (~14 nm compared to ~16 nm on November 09) implied  
 396 higher surface area and subsequently quicker growth. Since the aforementioned days featured  
 397 high SOA, the roles of photo-oxidation of VOCs in the formation and growth of nucleation mode  
 398 particles might reflect the very initial stages of SOA formation. However, to better understand  
 399 the relationships between SOA formation and the formation/growth of particles, data with higher  
 400 resolution and more comprehensive chemical information of SOA are crucially needed.



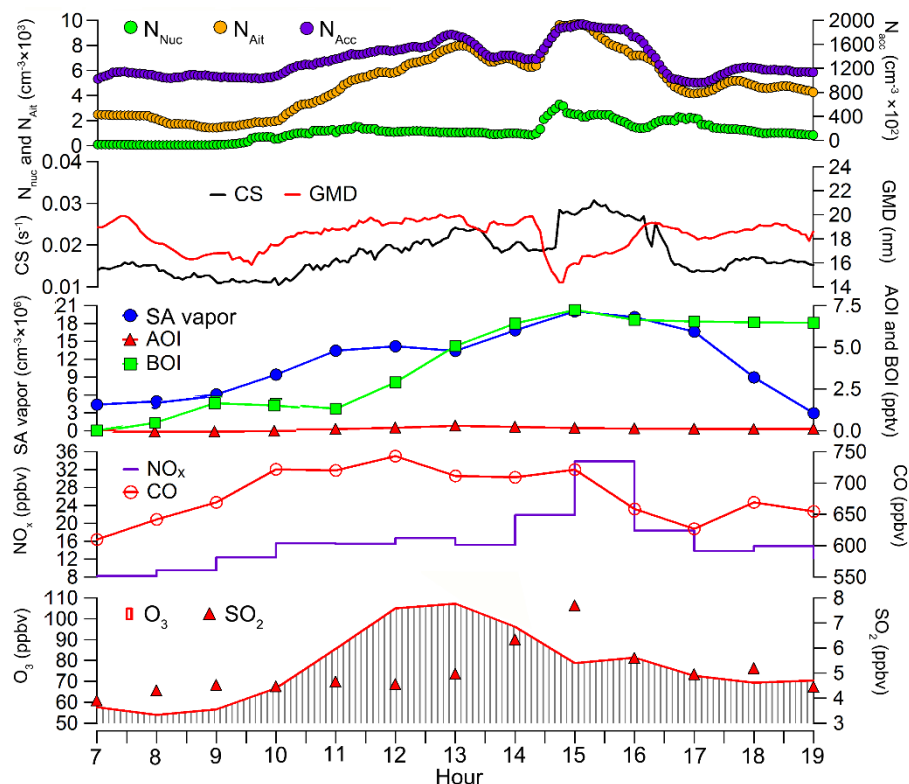
401  
 402 Figure 7 Evolutions of particle numbers, GMD of nucleation mode particles, CS, simulated SA  
 403 vapor, AOI, BOI and inorganic trace gases on October 31 (first sampling day of TMS12).



404  
 405 Figure 8 Evolutions of particle numbers, GMD of nucleation mode particles, CS, simulated SA vapor, AOI, BOI and inorganic trace gases on November 09 (second sampling day of TMS14).  
 406  
 407

408 Similarly, the growth of nucleation mode particles was also observed on November 19 (15:00-  
 409 16:00) (Figure 9). However, a distinct phenomenon was that the numbers of particles in  
 410 nucleation, Aitken and accumulation modes all showed rapid increases simultaneously from  
 411 around 14:30 and reached the highest values at ~15:00, which indicated that the particles in  
 412 different modes shared a common source. Although SO<sub>2</sub> and the simulated SA vapor began to  
 413 increase 1.5 hours earlier, this could not be a NPF event, as the increase of N<sub>Ait</sub> had no delay (no  
 414 banana shape) and the CS was high. In addition, the levels of primary air pollutants (*e.g.*, NO<sub>x</sub>  
 415 and CO) were high at the peak hours of all three-mode particle numbers. More importantly, we  
 416 found that CH<sub>3</sub>Cl largely increased from 13:00 to 15:00 and reached the maximum at 15:00 (see  
 417 Figure S6). Therefore, we suspected that biomass burning might be responsible for the increase  
 418 of particle numbers. This coincided with the high POC<sub>biomass burning</sub> (1.54 μg/m<sup>3</sup>) in PM<sub>2.5</sub> sample  
 419 collected on this day (TMS16). Generally, particles emitted from biomass burning are in Aitken  
 420 and accumulation modes (Reid et al., 2005). However, in vicinity of fire, nucleation mode can  
 421 also exist (Janhall et al., 2010). Here, although nucleation mode particles increased in the particle

422 burst event,  $N_{\text{nuc}}$  was very low (maximum= $2.1 \times 10^3 \text{ cm}^{-3}$ ), indicating that this was not a local  
 423 biomass burning and nucleation mode particles converted to larger size particles from the source  
 424 region to this site. This was also consistent with the regional influence on this day identified by  
 425 the wind fields (see section 3.3).



426  
 427 Figure 9 Evolutions of particle numbers, GMD of nucleation mode particles, CS, simulated SA  
 428 vapor, AOI, BOI and inorganic trace gases on November 19 (sampling day of TMS16).  
 429

#### 430 4. Conclusions

431  $\text{PM}_{2.5}$  samples were collected at a mountainous site in Hong Kong in autumn of 2010. Nine SOA  
 432 tracers in  $\text{PM}_{2.5}$  were analyzed, which helped to understand the compositions and sources of  
 433 SOC in this study. Results indicated that isoprene made the highest contribution to SOC  
 434 formation at this site, followed by monoterpenes, aromatics and sesquiterpenes. Averagely,  
 435 biogenic SOC dominated over anthropogenic SOC. However, anthropogenic SOC cannot be  
 436 neglected, particularly under the influences of regional transport (*e.g.*,  $1.2 \mu\text{g}/\text{m}^3$  in sample  
 437 TMS12) and/or local ship emission (*e.g.*,  $1.7 \mu\text{g}/\text{m}^3$  in sample TMS1). The simultaneous  
 438 observation of VOCs confirmed the role of aromatics in contributing to high concentrations of  
 439 anthropogenic SOC. In terms of SOC origins, regional transport caused nearly two-fold increase

440 of SOC, relative to local air. However, SOC load could also be significantly elevated by local  
441 ship emissions possibly containing abundant VOC precursors and SO<sub>2</sub>, which promoted SOC  
442 formation. In addition, the regional air was generally characterized with high biomass burning  
443 related POC, aggravating the PM<sub>2.5</sub>-bounded POC in Hong Kong. In combination with the SMPS  
444 data, we found that the formation of SOA (particularly the biogenic SOA) might be partially  
445 responsible for the new particle formation and growth of nucleation mode particles. Primary  
446 emissions, such as biomass burning, could cause particle burst events and lead to POC increases.  
447 To our knowledge, this is the first SOA study carried out in low-altitude (640 m) mountainous  
448 area of Hong Kong, where the air quality is under the combined influence of anthropogenic and  
449 biogenic emissions. This study also demonstrates the urgency of data acquisition with more  
450 comprehensive chemical information and higher time resolution in future SOA studies over this  
451 region.

#### 452 **Acknowledgements**

453 This study was supported by the Research Grants Council of the Hong Kong Special  
454 Administrative Region via grants CRF/C5004-15E, PolyU5154/13E, PolyU152052/14E, and  
455 CRF/C5022-14G, and the Hong Kong Polytechnic University PhD scholarships (project #RTUP).  
456 This study is partly supported by the Hong Kong PolyU internal grant (1-BBW4, 4-ZZFW, G-  
457 YBHT and 1-ZVJT) and by the Innovation and Technology Commission of the HKSAR via the  
458 Hong Kong Branch of National Rail Transit Electrification and Automation Engineering  
459 Technology Research Center (1-BBYD).

#### 460 **References**

461 Appel, B.R., Tokiwa, Y., Hsu, J., Kothny, E.L., and Hahn, E., 1985. Visibility as related to  
462 atmospheric aerosol constituents. *Atmos. Environ.* (1967), 19(9), 1525-1534.  
463 Birch, M.E., 1998. Analysis of carbonaceous aerosols: interlaboratory comparison. *Analyst*  
464 123(5), 851-857.  
465 Chameides, W.L., Yu, H., Liu, S.C., Bergin, M., Zhou, X., Mearns, L., Wang, G., Kiang, C.S.,  
466 Saylor, R.D., Luo, C., Huang, Y., Steiner, A., and Giorgi, F., 1999. Case study of the effects of  
467 atmospheric aerosols and regional haze on agriculture: An opportunity to enhance crop yields in  
468 China through emission controls?. *P. Natl. Acad. Sci.* 96(24), 13626-13633.

469 Claeys, M., Graham, B., Vas, G., Wang, W., Vermeylen, R., Pashynska, V., Cafmeyer, J., Guyon,  
470 P., Andreae, M., Artaxo, P., and Maenhaut, W., 2004. Formation of secondary organic aerosols  
471 through photooxidation of isoprene. *Science* 303(5661), 1173-1176.

472 Claeys, M., Szmigielski, R., Kourtchev, I., Van der Veken, P., Vermeylen, R., Maenhaut, W.,  
473 Jaoui, M., Kleindienst, T.E., Lewandowski, M., Offenberg, J.H. and Edney, E.O., 2007.  
474 Hydroxydicarboxylic acids: markers for secondary organic aerosol from the photooxidation of  $\alpha$ -  
475 pinene. *Environ. Sci. Technol.* 41(5), 1628-1634.

476 Ding, X., Wang, X.M., Gao, B., Fu, X.X., He, Q.F., Zhao, X.Y., Yu, J.Z., and Zheng, M., 2012.  
477 Tracer-based estimation of secondary organic carbon in the Pearl River Delta, south China. *J.*  
478 *Geophys. Res.: Atmos.* 117(D5), doi: 10.1029/2011JD016596.

479 Ding, X., Zhang, Y.Q., He, Q.F., Yu, Q.Q., Shen, R.Q., Zhang, Y.L., Zhang, Z., Lyu, S.J., Hu,  
480 Q.H., Wang, Y.S., Li, L.F., Song, W., and Wang, X.M., 2016. Spatial and seasonal variations of  
481 secondary organic aerosol from terpenoids over China. *J. Geophys. Res.: Atmos.* 121, doi:  
482 10.1002/2016JD025467.

483 Dockery, D.W., Pope, C.A., Xu, X., Spengler, J.D., Ware, J.H., Fay, M.E., Ferris Jr., B.G., and  
484 Speizer, F.E., 1993. An association between air pollution and mortality in six US cities. *New*  
485 *Engl. J. Med.* 329(24), 1753-1759.

486 Eddingsaas, N.C., Loza, C.L., Yee, L.D., Chan, M., Schilling, K.A., Chhabra, P.S., Seinfeld J.H.,  
487 and Wennberg, P.O., 2012.  $\alpha$ -pinene photooxidation under controlled chemical conditions-Part 2:  
488 SOA yield and composition in low-and high-NO<sub>x</sub> environments. *Atmos. Chem. Phys.* 12(16),  
489 7413-7427.

490 Forstner, H.J., Flagan, R.C., and Seinfeld, J.H., 1997. Secondary organic aerosol from the  
491 photooxidation of aromatic hydrocarbons: Molecular composition. *Environ. Sci. Technol.* 31(5),  
492 1345-1358.

493 Goldstein, A.H., Koven, C.D., Heald, C.L., and Fung, I.Y., 2009. Biogenic carbon and  
494 anthropogenic pollutants combine to form a cooling haze over the southeastern United States. *P.*  
495 *Natl. Acad. Sci.* 106(22), 8835-8840.

496 Guo, H., Jiang, F., Cheng, H.R., Simpson, I.J., Wang, X.M., Ding, A.J., Wang, T.J., Saunders,  
497 S.M., Wang, T., Lam, S.H.M., Blake, D.R., Zhang, Y.L., and Xie, M., 2009. Concurrent  
498 observations of air pollutants at two sites in the Pearl River Delta and the implication of regional  
499 transport. *Atmos. Chem. Phys.* 9(19), 7343-7360.



500 Guo, H., Lee, S.C., Louie, P.K., Ho, K.F., 2004. Characterization of hydrocarbons, halocarbons  
501 and carbonyls in the atmosphere of Hong Kong. *Chemosphere* 57(10):1363-72.

502 Guo, H., Ling, Z.H., Cheung, K., Jiang, F., Wang, D.W., Simpson, I.J., Barletta, B., Meinardi, S.,  
503 Wang, T.J., Saunders, S.M., and Blake, D.R., 2013. Characterization of photochemical pollution  
504 at different elevations in mountainous areas in Hong Kong. *Atmos. Chem. Phys.* 13(8), 3881-  
505 3898.

506 Guo, H., Ling, Z.H., Simpson, I.J., Blake, D.R., Wang, D.W., 2012b. Observations of isoprene,  
507 methacrolein (MAC) and methyl vinyl ketone (MVK) at a mountain site in Hong Kong. *J.*  
508 *Geophys. Res.: Atmos.* 16;117(D19), doi: 10.1029/2012JD017750.

509 Guo, H., So, K.L., Simpson, I.J., Barletta, B., Meinardi, S., and Blake, D.R., 2007. C<sub>1</sub>-C<sub>8</sub> volatile  
510 organic compounds in the atmosphere of Hong Kong: Overview of atmospheric processing and  
511 source apportionment. *Atmos. Environ.* 41(7), 1456-72.

512 Guo, H., Wang, D.W., Cheung, K., Ling, Z.H., Chan, C.K., and Yao, X.H., 2012a. Observation  
513 of aerosol size distribution and new particle formation at a mountain site in subtropical Hong  
514 Kong. *Atmos. Chem. Phys.* 12(20), 9923-9939.

515 Haddad, I.E., Marchand, N., Temime-Roussel, B., Wortham, H., Piot, C., Besombes, J.L.,  
516 Baduel, C., Voisin, D., Armengaud, A., and Jaffrezo, J.L., 2011. Insights into the secondary  
517 fraction of the organic aerosol in a Mediterranean urban area: Marseille. *Atmos. Chem. Phys.*  
518 11(5), 2059-2079.

519 Huang, J.P., Fung, J.C., and Lau, A.K., 2006. Integrated processes analysis and systematic  
520 meteorological classification of ozone episodes in Hong Kong. *J. Geophys. Res.: Atmos.*  
521 111(D20), doi: 10.1029/2005JD007012.

522 Ho, K.F., Lee, S.C., Guo, H., and Tsai, W.Y., 2004. Seasonal and diurnal variations of volatile  
523 organic compounds (VOCs) in the atmosphere of Hong Kong. *Sci. Total Environ.* 322(1):155-  
524 166.

525 Hu, D., Bian, Q., Li, T.W., Lau, A. K., and Yu, J.Z., 2008. Contributions of isoprene,  
526 monoterpenes,  $\beta$ -caryophyllene, and toluene to secondary organic aerosols in Hong Kong during  
527 the summer of 2006. *J. Geophys. Res.: Atmos.* 113(D22), doi: 10.1029/2008JD010437.

528 Jang, M., Carroll, B., Chandramouli, B., and Kamens, R.M., 2003. Particle growth by acid-  
529 catalyzed heterogeneous reactions of organic carbonyls on preexisting aerosols. *Environ. Sci.*  
530 *Technol.* 37(17), 3828-3837.

531 Jang, M., Czoschke, N.M., Lee, S., and Kamens, R.M., 2002. Heterogeneous atmospheric  
532 aerosol production by acid-catalyzed particle-phase reactions. *Science*, 298(5594), 814-817.

533 Janhall, S., Andreae, M.O., and Poschl, U., 2010. Biomass burning aerosol emissions from  
534 vegetation fires: particle number and mass emission factors and size distributions. *Atmos. chem.*  
535 *Phys.* 10(3), 1427-1439.

536 Kleindienst, T.E., Jaoui, M., Lewandowski, M., Offenberg, J.H., Lewis, C.W., Bhave, P.V., and  
537 Edney, E.O., 2007. Estimates of the contributions of biogenic and anthropogenic hydrocarbons  
538 to secondary organic aerosol at a southeastern US location. *Atmos. Environ.* 41(37), 8288-8300.

539 Kroll, J.H., Ng, N.L., Murphy, S.M., Flagan, R.C., and Seinfeld, J.H., 2006. Secondary organic  
540 aerosol formation from isoprene photooxidation. *Environ. Sci. Technol.* 40(6), 1869-1877.

541 Lee, S., Kim, H.K., Yan, B., Cobb, C.E., Hennigan, C., Nichols, S., Chamber, M., Edgerton, E.S.,  
542 Jansen, J.J., Hu, Y., Zheng, M., Weber, R., and Russell, A.G., 2008. Diagnosis of aged  
543 prescribed burning plumes impacting an urban area. *Environ. Sci. Technol.* 42(5), 1438-1444.

544 Lewandowski, M., Jaoui, M., Offenberg, J.H., Kleindienst, T.E., Edney, E.O., Sheesley, R.J., and  
545 Schauer, J.J. (2008). Primary and secondary contributions to ambient PM in the midwestern  
546 United States. *Environ. Sci. Technol.* 42(9), 3303-3309.

547 Ling, Z.H., Guo, H., Lam, S.H.M., Saunders, S.M., and Wang, T., 2014. Atmospheric  
548 photochemical reactivity and ozone production at two sites in Hong Kong: Application of a  
549 Master Chemical Mechanism–photochemical box model. *J. Geophys. Res.: Atmos.* 119(17),  
550 10567-10582.

551 Maria, S.F., Russell, L.M., Gilles, M.K., and Myneni, S.C., 2004. Organic aerosol growth  
552 mechanisms and their climate-forcing implications. *Science*, 306(5703), 1921-1924.

553 Offenberg, J.H., Lewandowski, M., Jaoui, M., and Kleindienst, T.E., 2011. Contributions of  
554 biogenic and anthropogenic hydrocarbons to secondary organic aerosol during 2006 in Research  
555 Triangle Park, NC. *Aerosol Air Qual. Res.* 11(2), 99-108.

556 Offenberg, J.H., Lewis, C.W., Lewandowski, M., Jaoui, M., Kleindienst, T.E., and Edney, E.O.,  
557 2007. Contributions of toluene and  $\alpha$ -pinene to SOA formed in an irradiated toluene/ $\alpha$ -  
558 pinene/NO<sub>x</sub>/air mixture: Comparison of results using <sup>14</sup>C content and SOA organic tracer  
559 methods. *Environ. Sci. Technol.* 41(11), 3972-3976.

560 Pope III, C.A., and Dockery, D.W., 2006. Health effects of fine particulate air pollution: lines  
561 that connect. *J. Air Waste Manage. Assoc.* 56(6), 709-742.

562 Reda, A.A., Schnelle-Kreis, J., Orasche, J., Abbaszade, G., Lintelmann, J., Arteaga-Salas, J.M.,  
563 Stengel, B., Rade, R., Harndorf, H., Sippula, O., Streibel, T., and Zimmermann, R., 2014. Gas  
564 phase carbonyl compounds in ship emissions: Differences between diesel fuel and heavy fuel oil  
565 operation. *Atmos. Environ.* 94, 467-478.

566 Reid, J.S., Koppmann, R., Eck, T.F., and Eleuterio, D.P., 2005. A review of biomass burning  
567 emissions part II: intensive physical properties of biomass burning particles. *Atmos. Chem. Phys.*  
568 5(3), 799-825.

569 Rudolph, J., Khedim, A., Koppmann, R., and Bonsang, B., 1995. Field study of the emissions of  
570 methyl chloride and other halocarbons from biomass burning in western Africa. *J. Atmos. Chem.*  
571 22(1-2), 67-80.

572 Sippula, O., Stengel, B., Sklorz, M., Streibel, T., Rabe, R., Orasche, J., Lintelmann, J., Michalke,  
573 B., Abbaszade, G., Radischat, C., Groger, T., Schnelle-Kreis, J., Harndorf, H., and Zimmermann,  
574 R., 2014. Particle emissions from a marine engine: chemical composition and aromatic emission  
575 profiles under various operating conditions. *Environ. Sci. Technol.* 48(19), 11721-11729.

576 So, K.L., and Wang, T., 2003. On the local and regional influence on ground-level ozone  
577 concentrations in Hong Kong. *Environ. Pollut.* 123(2), 307-317.

578 Stocker, T.F., Qin, D., Plattner, G.K., et al. IPCC, 2013: climate change 2013: the physical  
579 science basis. Contribution of working group I to the fifth assessment report of the  
580 intergovernmental panel on climate change [J]. 2013.

581 Surratt, J.D., Lewandowski, M., Offenberg, J.H., Jaoui, M., Kleindienst, T.E., Edney, E.O., and  
582 Seinfeld, J.H., 2007. Effect of acidity on secondary organic aerosol formation from isoprene.  
583 *Environ. Sci. Technol.* 41(15), 5363-5369.

584 Volkamer, R., Jimenez, J.L., San Martini, F., Dzepina, K., Zhang, Q., Salcedo, D., Molina, L.T.,  
585 Worsnop, D.R., and Molina, M.J., 2006. Secondary organic aerosol formation from  
586 anthropogenic air pollution: Rapid and higher than expected. *Geophys. Res. Lett.* 33(17), doi:  
587 10.1029/2006GL026899.

588 Williams, B.J., Jayne, J.T., Lambe, A.T., Hohaus, T., Kimmel, J.R., Sueper, D., Brooks, W.,  
589 Williams, L.R., Trimborn, A.M., Martinez, R.E., Hayes, P.L., Jimenez, J.L., Kreisberg, N.M.,  
590 Hering, S.V., Worton, D.R., Goldstein, A.H., and Worsnop, D.R., 2014. The first combined  
591 thermal desorption aerosol gas chromatograph-aerosol mass spectrometer (TAG-AMS). *Aerosol*  
592 *Sci. Technol.* 48(4), 358-370.

1 **Observation of SOA tracers at a mountainous site in Hong Kong: chemical characteristics,**  
2 **origins and implication on particle growth**

3 X.P. Lyu <sup>1</sup>, H. Guo <sup>1\*</sup>, H.R. Cheng <sup>2\*\*</sup>, X.M. Wang <sup>3</sup>, X. Ding <sup>3</sup>, H.X. Lu <sup>1</sup>, D.W. Yao <sup>1</sup>, and C.  
4 Xu <sup>1</sup>

5 <sup>1</sup> Department of Civil and Environmental Engineering, The Hong Kong Polytechnic University,  
6 Hong Kong

7 <sup>2</sup> Department of Environmental Engineering, School of Resource and Environmental Sciences,  
8 Wuhan University, Wuhan, China

9 <sup>3</sup> State Key Laboratory of Organic Geochemistry, Guangzhou Institute of Geochemistry, Chinese  
10 Academy of Sciences, Guangzhou, China

11 Corresponding author: H. Guo ([ceguohai@polyu.edu.hk](mailto:ceguohai@polyu.edu.hk)); H.R. Cheng ([chenghr@whu.edu.cn](mailto:chenghr@whu.edu.cn))

12

13 **Abstract:** Secondary organic aerosol (SOA) is an important constituent of airborne fine particles.  
14 PM<sub>2.5</sub> (particles with aerodynamic diameters  $\leq 2.5 \mu\text{m}$ ) samples were collected at a mountainous  
15 site in Hong Kong in autumn of 2010, and analyzed for SOA tracers. Results indicated that the  
16 concentrations of isoprene SOA tracers ( $54.7 \pm 22.7 \text{ ng/m}^3$ ) and aromatics SOA tracers ( $2.1 \pm 1.6$   
17  $\text{ng/m}^3$ ) were on relatively high levels in Hong Kong. Secondary organic carbon (SOC) derived  
18 from isoprene, monoterpenes, sesquiterpenes and aromatics was estimated with the SOA tracer  
19 based approach, which constituted  $0.35 \pm 0.15 \mu\text{g/m}^3$  ( $40.6 \pm 5.7\%$ ),  $0.20 \pm 0.03 \mu\text{g/m}^3$  ( $30.4 \pm 5.5\%$ ),  
20  $0.05 \pm 0.02 \mu\text{g/m}^3$  ( $5.6 \pm 1.7\%$ ) and  $0.26 \pm 0.20 \mu\text{g/m}^3$  ( $21.3 \pm 8.2\%$ ) of the total estimated SOC.  
21 Biogenic SOC ( $0.60 \pm 0.18 \mu\text{g/m}^3$ ) dominated over anthropogenic SOC ( $0.26 \pm 0.20 \mu\text{g/m}^3$ ) at this  
22 site. In addition to the total estimated SOC ( $17.8 \pm 4.6\%$  of organic carbon (OC) in PM<sub>2.5</sub>),  
23 primary organic carbon (POC) emitted from biomass burning also accounted for a considerable  
24 proportion of OC ( $11.6 \pm 3.2\%$ ). Insight into the OC origins found that regional transport  
25 significantly ( $p < 0.05$ ) elevated SOC from  $0.37 \pm 0.17$  to  $1.04 \pm 0.39 \mu\text{g/m}^3$ . Besides, SOC load  
26 could also increase significantly if there was influence from local ship emission. Biomass  
27 burning related POC in regional air masses ( $0.81 \pm 0.24 \mu\text{g/m}^3$ ) was also higher ( $p < 0.05$ ) than that  
28 in samples affected by local air ( $0.29 \pm 0.35 \mu\text{g/m}^3$ ). Evidences indicated that SOA formation was  
29 closely related to new particle formation and the growth of nucleation mode particles, while  
30 biomass burning was responsible for some particle burst events in Hong Kong. This is the first  
31 SOA study in afforested areas of Hong Kong.

32 **Keywords:** Secondary organic aerosol, SOA tracer, biogenic SOA, regional transport, particle  
33 growth

## 34 **1. Introduction**

35 Atmospheric aerosol has been well recognized to affect global climate change (Stocker et al.,  
36 2013), human health (Dockery et al., 1993; Pope III and Dockery, 2006), visibility (Appel et al.,  
37 1985) and sustainability of economy (Chameides et al., 1999). Secondary organic aerosol (SOA)  
38 has been identified to play critical roles in these effects (Maria et al., 2004; Volkamer et al., 2006;  
39 Baltensperger et al., 2008), thus receiving sufficient attentions in recent years.

40 So far, the scientific community has reached a consensus that volatile organic compounds (VOCs)  
41 from biogenic emissions and anthropogenic aromatics are key precursors of SOA (Forstner et al.,  
42 1997; Claeys, et al., 2004). In global scale, biogenic SOA is thought to be the greatest constituent  
43 of SOA, due to the worldwide largest emission of biogenic VOCs (*e.g.*, isoprene, monoterpenes  
44 and sesquiterpenes) and formation of biogenic SOA spanning a wide range of conditions (the  
45 level of NO<sub>x</sub>, humidity and aerosol acidity) (Kroll et al., 2006). However, anthropogenic SOA  
46 has also been found to be significant in urban areas (Volkamer et al., 2006). Furthermore, upon  
47 the findings that biogenic SOA correlates well with the indicators of anthropogenic emissions  
48 (Goldstein et al., 2009; Hoyle et al., 2011), it is believed that man-made air pollutants promote  
49 the formation of biogenic SOA, in addition to serving as SOA precursors themselves. These  
50 promoting effects at least include forming aerosol seeds, catalyzing photooxidation and  
51 transformation of biogenic VOCs and their oxidation products and changing the reaction  
52 pathways (*e.g.*, atmospheric fate of isoprene in low- and high-NO<sub>x</sub> environments) (Hoyle et al.,  
53 2011). It is believed that SOA is a collection of hundreds to thousands of organic chemicals  
54 featuring relatively low volatilities. To understand SOA formation and explore the potential  
55 sources, SOA speciation is of great necessity. However, due to the difficulty in chemical analysis  
56 of SOA tracers, the chemical compositions of SOA are far from being well understood. The  
57 traditional analysis by gas chromatography-mass spectrometer detector (GC-MSD) generally  
58 quantifies a total of less than 20 organic compounds in particles (Offenberg et al., 2007;  
59 Kleindienst et al., 2007). Although some advanced instruments have been developed nowadays,  
60 such as aerosol mass spectrometry and thermal desorption aerosol gas chromatography, they are  
61 either fragment-based or highly dependent upon the skills and knowledge of users (Williams et

62 al., 2014). Instead, SOA tracer based approach is a simplified method widely used to estimate the  
63 amount, precursors and sources of SOA (Kleindienst et al., 2007; Ding et al., 2012).

64 The SOA tracer based approach applies the laboratory obtained ratios between the sum of  
65 specific SOA tracers and total mass of SOA (or secondary organic carbon (SOC)) produced from  
66 individual (group of) species to the field measured SOA tracers (Kleindienst et al., 2007),  
67 roughly estimating SOA (SOC) derived from an individual VOC or VOC group. Table S1  
68 summarizes the VOC precursors, corresponding SOA tracers and the ratios between SOA tracers  
69 and SOA (or SOC), as reported by Kleindienst et al. (2007). The drawbacks of this method are  
70 obvious. For instance, it is controversial whether the laboratory obtained ratios can be directly  
71 applied to the field measured SOA tracers. However, it provides a feasible approach to estimate  
72 the SOA concentration, which is especially helpful in the cases of not well knowing the SOA  
73 compositions. More importantly, Offenberg et al. (2007) confirmed that the SOA tracer based  
74 approach was reliable through comparing with the results obtained from  $^{14}\text{C}$  contents.

75 Hong Kong, one of the most developed regions in East Asia, has a total territory area of  
76  $\sim 1.1 \times 10^3 \text{ km}^2$  and a total population of  $\sim 7$  million. Despite high population density, it keeps 24  
77 country parks and a vegetation coverage rate of 70%. Evergreen broadleaf trees are common in  
78 Hong Kong. Guenther et al. (2006) suggested that shrubs are large emitters of isoprene, a typical  
79 and most abundant biogenic VOC. The total emission amount of biogenic VOCs in Hong Kong  
80 is estimated as  $8.6 \times 10^3 \text{ ton C/a}$  (Tsui et al., 2009). Field measurements also revealed that  
81 isoprene in Hong Kong is relatively high (300-400 pptv) (Guo et al., 2007, 2012a). In contrast,  
82 aromatics are largely emitted from vehicular exhaust and solvent usage in Hong Kong. For  
83 example, toluene is one of the most abundant aromatics, with the level of 3-6 ppbv (Guo et al.,  
84 2004; Ho et al., 2004). Therefore, local emission of VOCs has a great potential forming SOA in  
85 Hong Kong. In addition to local SOA formation, regional transport is inevitable due to severe air  
86 pollution in upwind direction of Hong Kong (*i.e.*, inland Pearl River Delta (PRD) region).  
87 Studies confirmed that Hong Kong received SOA produced by isoprene and toluene from inland  
88 PRD region (Hu et al., 2008). However, the previous SOA studies in Hong Kong all focused on  
89 urban areas, which are not enough to understand the abundance, compositions and sources of  
90 SOA in low-altitude mountainous area where both anthropogenic and biogenic emissions are  
91 important.



92 In this study, SOC derived from isoprene, monoterpenes, sesquiterpenes and aromatics at a  
93 mountainous site in Hong Kong were estimated using a SOA tracer based approach. Local and  
94 regional contributions to SOC and biomass burning related POC were determined. Furthermore,  
95 in combination with particle size distribution simultaneously monitored by a scanning mobility  
96 particle sizer (SMPS), the relationships between SOA formation and particle growth were  
97 examined.

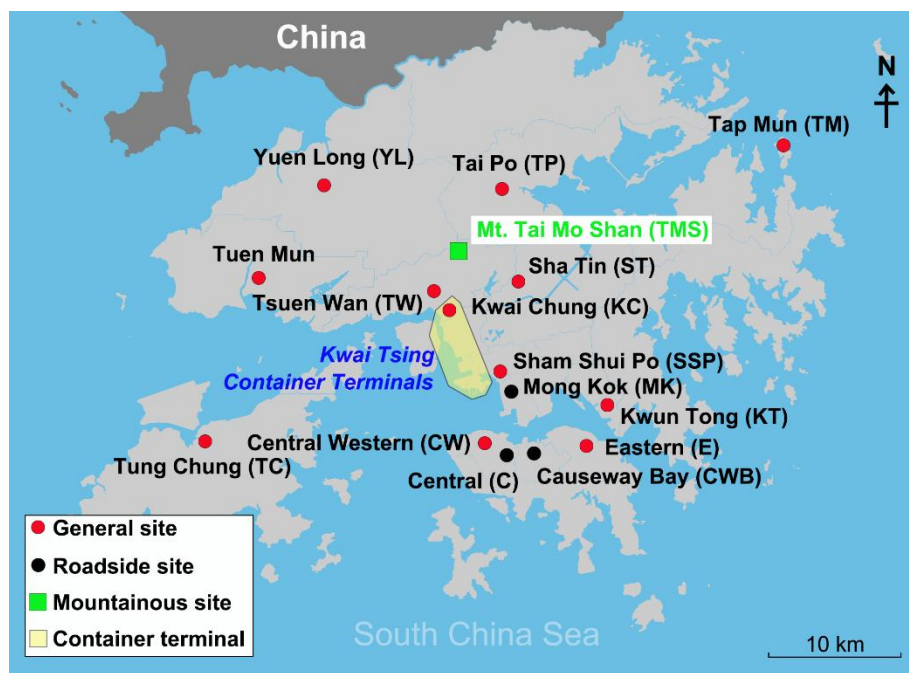
## 98 **2. Methodology**

### 99 **2.1 Sample collection**

100 Hong Kong, a coastal city surrounded by the South China Sea (SCS) to the east and south, is  
101 located in southern China. Under the dominance of subtropical monsoon climate, Hong Kong  
102 receives northerly winds originating from the heavily polluted PRD region in cool seasons  
103 (October-March), while prevailing southerly winds bring in clean air from SCS in warm seasons  
104 (April-August) (So and Wang, 2003). The sampling site (22.405° N, 114.118° E, 640 m a.s.l) was  
105 set up at the mountainside of the highest mountain in Hong Kong (Mt. Tai Mo Shan with the  
106 maximum altitude of 957 m, TMS). The vegetation on this mountain mainly includes *Acacia*  
107 *confusa*, *Lophotemon confertus*, *Machilus chekiangensis* and *Schima superba* below 550 m,  
108 while it turns to shrubs and grasses above 550 m (Guo et al., 2012b). As demonstrated in  
109 previous studies (Guo et al., 2013; Ling et al., 2014), regional transport of air pollutants from  
110 inland PRD, mesoscale circulation (mountain-valley breezes) and in situ atmospheric chemistry  
111 are the main processes that significantly influence air quality at this site. Figure 1 shows the  
112 geographical locations of the sampling site and air quality monitoring stations (AQMSs) of Hong  
113 Kong Environmental Protection Department (HKEPD).

114 From September 7 to November 26, 2010, a total of 19 PM<sub>2.5</sub> samples were collected. The  
115 instrument was an Anderson high volume PM<sub>2.5</sub> sampler, with a flow rate of 750 L/min. Pre-  
116 baked A4 size quartz fiber filters were used to collect the samples, which were stored in the  
117 refrigerator at -18 °C after sampling. Generally, each filter sampling lasted for 45-55 hours,  
118 except for the cases that the instrument stopped abnormally on some days due to thunderstorm-  
119 caused power outages. Table S2 lists the sample IDs, start and end dates & times. The origins of  
120 air masses, as distinguished by wind field and ratio of SO<sub>2</sub>/NO<sub>x</sub> (see section 3.3 for details), are  
121 also shown in the table. Additionally, the particle number concentrations and size distributions in  
122 the size range of 5.5-350.4 nm in 44 size bins were monitored by a scanning mobility particle

123 sizer (SMPS) from October 27 to November 29. Detailed introductions about the operation  
124 procedures of SMPS and data processing can be found in Guo et al. (2012a). We also collected  
125 ambient VOC samples during September 28-November 21. Inorganic trace gases (SO<sub>2</sub>, CO, NO,  
126 NO<sub>2</sub> and O<sub>3</sub>) and weather conditions were measured simultaneously with the PM<sub>2.5</sub> sampling.  
127 Details about VOC sampling, VOC analysis and monitoring of trace gases are provided in Guo et  
128 al. (2013) and Ling et al. (2014).



129  
130 Figure 1 Geographic locations of the sampling site (TMS), AQMSs of HKEPD and the container  
131 terminal area where nine container terminals are located. Capital letters in the brackets are  
132 abbreviations of the site/stations

## 133 134 2.2 Chemical analysis

135 OC and element carbon (EC) in PM<sub>2.5</sub> samples were analyzed using the thermo-optical  
136 transmittance method recommended by National Institute for Occupational Safety and Health  
137 (NIOSH) (Birch, 1998). The concentrations of OC and EC are shown in Figure S1.

138 The method of SOA analysis was in line with that introduced by Ding et al. (2011). Briefly, the  
139 procedures for each sample include solvent extraction, derivation, analysis by GC-MSD, and  
140 identification and quantification of SOA tracers. 1/8 of each filter was extracted three times by  
141 sonication in the solvent of 40 mL of 1:1 (v/v) dichloride methane (DCM)/methanol mixture.  
142 Prior to extraction, the internal standards (hexadecanoic acid-D<sub>31</sub>, phthalic acid-D<sub>4</sub> and

143 levoglucosan-<sup>13</sup>C<sub>6</sub>) were spiked into the samples. The three-time extracts of each sample were  
144 combined, filtered and concentrated to ~2 mL, which was further divided into two parts for  
145 methylation and silylation derivation, respectively. In methylation derivation, the extract  
146 experienced a gentle nitrogen blow to dryness, and subsequent addition of 200 μL of DCM, 10  
147 μL of methanol and 300 μL of freshly prepared diazomethane. Then, it was kept in room  
148 temperature for one hour to derivatize acids to methyl esters, after which the sample was blown  
149 to 200 μL and used for analysis of some α-pinene SOA tracers (Pinonic acid, pinic acid and 3-  
150 methyl-1,2,3-butanetricarboxylic acid). The silylation reagent was 100 μL of pyridine and 200  
151 μL of N,O-bis-(trimethylsilyl)-trifluoroacetamide (BSTFA) plus 1% trimethylchlorosilane  
152 (TMCS). Differently, the derivation was carried out in an oven at 70 °C for one hour. One α-  
153 pinene SOA tracer (3-hydroxyglutanic acid) and tracers for isoprene SOA, sesquiterpenes SOA,  
154 and toluene SOA were analyzed from the silylated sample. An Agilent 5973N GC/MSD was  
155 employed to do the analysis. The identification of SOA tracers was based on the comparison of  
156 mass spectra with previous studies, and their retention time in GC chromatogram with other  
157 known compounds as the references. Pinonic acid and pinic acid were quantified by authentic  
158 standards. However, due to lack of standards, other α-pinene SOA tracers, isoprene SOA tracers,  
159 β-Caryophyllenic acid and 2,3-dihydroxy-4-oxopentanoic acid were quantified using pinic acid  
160 (PA), erythritol, octadecanoic acid and azelaic acid, respectively. The detection limits (DLs) for  
161 pinonic acid, pinic acid, erythritol, octadecanoic acid and azelaic acid were 0.05, 0.07, 0.06, 0.09,  
162 and 0.11 ng/m<sup>3</sup>, respectively. Levoglucosan was also quantified with the DL of 0.15 ng/m<sup>3</sup>. The  
163 SOA tracers analyzed in this study are highlighted in Table S1.

### 164 **2.3 Quality assurance and quality control**

165 In this study, internal standards were not spiked on the filters before sampling, to avoid their  
166 influences on OC analysis. According to the saturation concentrations of SOA tracers calculated  
167 by Ding et al. (2016), SOA tracers analyzed in this study were of low volatilities, except for  
168 pinonic acid. Therefore, pinonic acid in airborne PM<sub>2.5</sub> might be underestimated due to the blow-  
169 off effect during sampling, which however should not be significant to other SOA tracers.  
170 Recovery target compounds were spiked in the samples before analysis of SOA tracers. The  
171 recovery rates were 104±2%, 68±13%, 62±14%, 78±10%, 81±9% and 87±4% for pinonic acid,  
172 pinic acid, erythritol, octadecanoic acid, azelaic acid and levoglucosan, respectively. Since

173 internal standards were added into the samples prior to analysis, we did not use the recovery  
174 rates to correct the concentrations of SOA tracers.

## 175 **2.4 Processing of SMPS data**

176 In this study, particles measured by SMPS were divided into nucleation (5.5-24.7 nm), Aitken  
177 (24.7-101.4 nm) and accumulation modes (101.4-350.4 nm). Geometric mean diameter (GMD)  
178 for nucleation mode particles (5.5-24.7 nm) was calculated using the following equations (Guo et  
179 al., 2012a).

$$180 \text{GRs} = \frac{d_{\text{GMD}}}{d_t} \quad (\text{Equation (1)})$$

$$181 \text{GMD} = e^{(\sum n_i \ln d_i)/N} \quad (\text{Equation (2)})$$

$$182 \frac{d_N}{d_{\log D_p^2}} = \frac{\Delta N}{\log D_p^2 - \log D_p^1} \quad (\text{Equation (3)})$$

183 where  $n_i$  is the particle number concentration in the  $i^{\text{th}}$  bin with upper diameter of  $d_i$ ,  $N$  represents  
184 the total number concentration ( $\text{cm}^{-3}$ ).  $\Delta N$  is the particle number concentration in the size bin  
185 with upper and lower limit diameter of  $D_p^2$  and  $D_p^1$ , respectively.

186 Condensation sink (CS), which describes the loss rate of vapor molecules and newly formed  
187 particles on the pre-existing aerosol particles, was calculated as follows (Kulmala et al., 2005):

$$188 \text{CS} = 2\pi D \int D_p \beta_m(D_p) n(D_p) dD_p = 2\pi D \sum_i \beta_{mi} D_{pi} N_i \quad (\text{Equation (4)})$$

189 where  $D$  is the diffusion coefficient of the condensing vapor,  $\beta_m$  is the transitional regime  
190 correction factor,  $D_p$  denotes the particle diameter,  $n$  and  $N$  represent the particle numbers.  $\beta_{mi}$ ,  
191  $D_{pi}$  and  $N_i$  are the specific values for a given size bin ( $i$ ). Growth factor calculated according to  
192 Laakso et al. (2004) was used to calibrate the dry particle size measured by SMPS.

193

## 194 **3. Results and discussion**

### 195 **3.1 Concentrations of SOA tracers**

196 Table 1 shows the average concentrations of SOA tracers derived from different precursors at  
197 TMS. Isoprene SOA tracers were the most abundant ( $54.7 \pm 22.7 \text{ ng/m}^3$ ), followed by the tracers  
198 generated from monoterpenes ( $26.3 \pm 4.5 \text{ ng/m}^3$ ), aromatics ( $2.1 \pm 1.6 \text{ ng/m}^3$ ) and sesquiterpenes  
199 ( $1.1 \pm 0.4 \text{ ng/m}^3$ ). Figure 2 compares the concentrations of SOA tracers between previous studies  
200 and the present study. The number and species of SOA tracers for the same precursor were the  
201 same. For the cases that total concentration of monoterpenes SOA tracers was given (*e.g.*,  
202 Offenberg et al., 2011), a factor was applied to the total concentration to roughly estimate the

203 sum of monoterpenes SOA tracers with the number and species identical to this study (see  
204 section S1 and Figure S2 in the Supplement). It was found that isoprene SOA tracers at TMS  
205 were on relatively high level ( $54.7 \pm 22.7 \text{ ng/m}^3$ ), comparable to or even higher than those  
206 detected in the forest ( $61.4 \pm 30.4 \text{ ng/m}^3$  in Kleindienst et al. (2007) and  $39.0 \pm 17.2 \text{ ng/m}^3$  in  
207 Offenberg et al. (2011)). In fact, isoprene at TMS was relatively low (2-517 pptv), the high  
208 isoprene SOA tracers indicated that biogenic SOA formation at this site might be enhanced by  
209 anthropogenic emissions, *e.g.*, sufficient aerosol seeds from SO<sub>2</sub>-related new particle formation  
210 (Guo et al., 2012a). Certainly, regional transport could also contribute to high isoprene SOA  
211 tracers, as reported by Hu et al. (2008). For the anthropogenic SOA, the tracer produced by  
212 aromatics (2,3-dihydroxy-4-oxopentanoic acid) was noticeable. Although the average 2,3-  
213 dihydroxy-4-oxopentanoic acid in this study ( $2.1 \pm 1.6 \text{ ng/m}^3$ ) was not significantly higher than  
214 that in other studies ( $p > 0.05$ ), its maximum value reached  $13.5 \text{ ng/m}^3$ . Given abundant aromatics  
215 in the atmosphere of Hong Kong and mesoscale circulations between TMS and the surrounding  
216 urban areas, local formation could be an important factor contributing to high aromatics SOA at  
217 TMS. Moreover, it was reported that 2,3-dihydroxy-4-oxopentanoic acid at an urban  
218 background site in inland PRD was very high ( $13.1 \text{ ng/m}^3$ ) (Ding et al., 2012). Hence, regional  
219 transport might be partially responsible for the relatively high aromatics SOA tracer in Hong  
220 Kong. SOA tracers derived from monoterpenes and sesquiterpenes were on moderate levels,  
221 compared to other studies.

222 3-Methyl-1,2,3-butanetricarboxylic acid and 3-hydroxyglutanic acid, formed from monoterpenes  
223 oxidation in the presence of NO<sub>x</sub> (Claeys et al., 2007; Eddingsaas et al., 2012), dominated the  
224 measured monoterpenes SOA tracers, consistent with those at an urban background site in inland  
225 PRD (Ding et al., 2012). Pinonic acid and pinic acid, formed from OH oxidation of  $\alpha$ -pinene in  
226 NO<sub>x</sub> free environment or ozonolysis of  $\alpha$ -pinene (Eddingsaas et al., 2012), were also higher than  
227 those in urban areas of Hong Kong (almost below DLs) (Hu et al., 2008). Since NO<sub>x</sub> was at the  
228 magnitude of several ppbv, the higher pinonic acid and pinic acid were likely due to the higher  
229 O<sub>3</sub> ( $69.2 \pm 2.4 \text{ ppbv}$  at TMS and  $30.8 \pm 2.6 \text{ ppbv}$  at the mountain foot) at this mountainous site. In  
230 addition, other tracers including 3-hydroxy-4,4-dimethylglutaric acid, 3-isopropylpentanedioic  
231 acid, 3-acetylpentanedioic acid and 3-acetylhexanedioic acid, which were not measured in this  
232 study, accounted for  $46.9 \pm 4.0\%$  of the total amount of tracers according to Kleindienst et al.  
233 (2007). Of the isoprene SOA tracers, 2-methylthreitol and 2-methylerythritol are representative

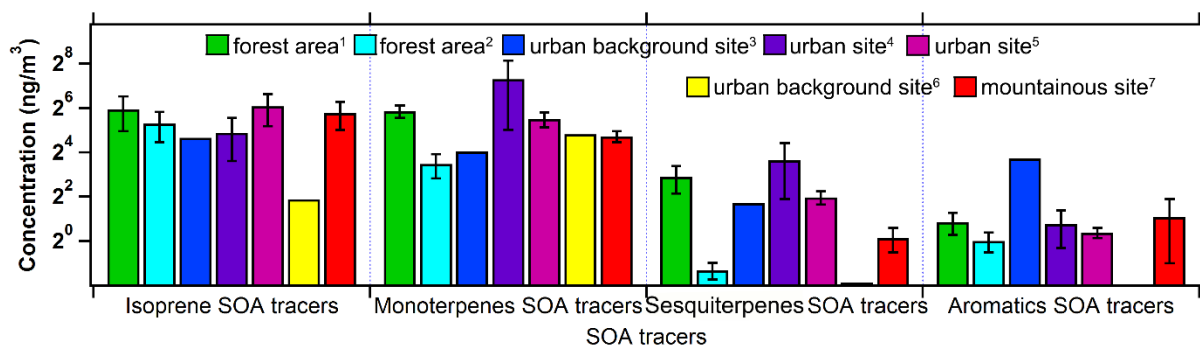
234 products formed through the photooxidation of isoprene hydroxyhydroperoxides and acid  
 235 catalysis of epoxydiols of isoprene in low NO<sub>x</sub> environment when RO<sub>2</sub> reacting with HO<sub>2</sub>  
 236 dominated the loss of RO<sub>2</sub> (Claeys et al., 2004; Surratt et al., 2010). In this study, they accounted  
 237 for 83.5±8.1% of the total isoprene tracers. However, NO<sub>x</sub> was not low enough and RO<sub>2</sub> reacting  
 238 with NO was the main sink of RO<sub>2</sub> (Ling et al., 2014), implying that other mechanisms might  
 239 enhance the formation of 2-methyltetrols (sum of 2-methylthreitol and 2-methylerythritol) at this  
 240 site, such as acid catalysis (Surratt et al., 2007).

241 Table 1 Average concentrations of SOA tracers derived from monoterpenes, isoprene,  
 242 sesquiterpenes and aromatics (mean±95% confidence interval (C.I.)).

VOC precursor	SOA tracer	Concentration (ng/m <sup>3</sup> )
Monoterpenes	Pinonic acid	1.2±0.4
	Pinic acid	2.0±0.6
	3-methyl-1,2,3-butanetricarboxylic acid	16.0±3.5
	3-hydroxyglutanic acid	7.1±2.7
	Sum 1	26.3±4.5
Isoprene	2-Methylthreitol	14.7±6.6
	2-Methylerythritol	31.2±13.1
	2-methylglyceric acid	5.2±3.1
	cis-2-Methyl-1,3,4-trihydroxy-1-butene	0.8±0.5
	trans-2-Methyl-1,3,4-trihydroxy-1-butene	2.0±1.3
	3-Methyl-2,3,4-trihydroxy-1-butene	0.7±0.3
	Sum 2	54.7±22.7
Sesquiterpenes	β-Caryophyllenic acid	1.1±0.4
Aromatics	2,3-Dihydroxy-4-oxopentanoic acid	2.1±1.6

243





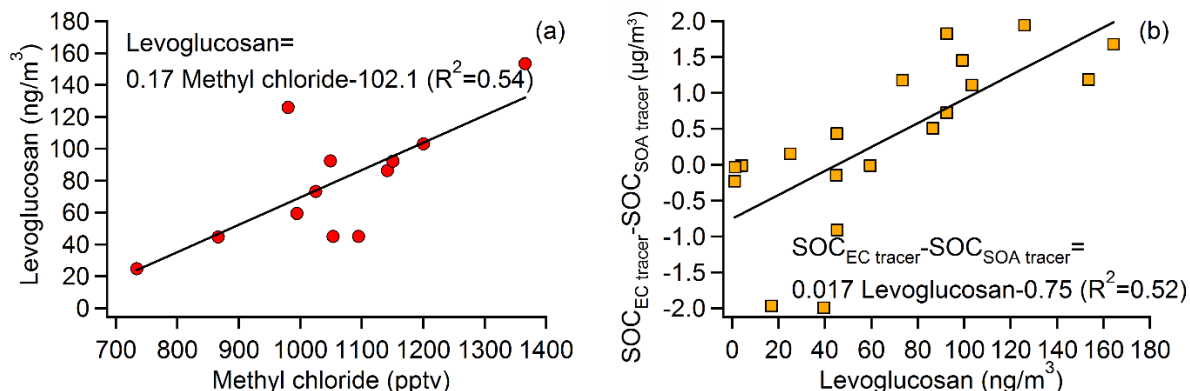
244  
 245 Figure 2 Comparison of SOA tracers between previous studies and this study. <sup>1</sup>Kleindienst et al.  
 246 (2007); <sup>2</sup>Offenberg et al. (2011); <sup>3</sup>Ding et al. (2012); <sup>4</sup>Hu et al. (2008); <sup>5</sup>Lewandowski et al.  
 247 (2008); <sup>6</sup>Haddad et al. (2011); <sup>7</sup>this study.

248  
 249 **3.2 Estimate of SOC**

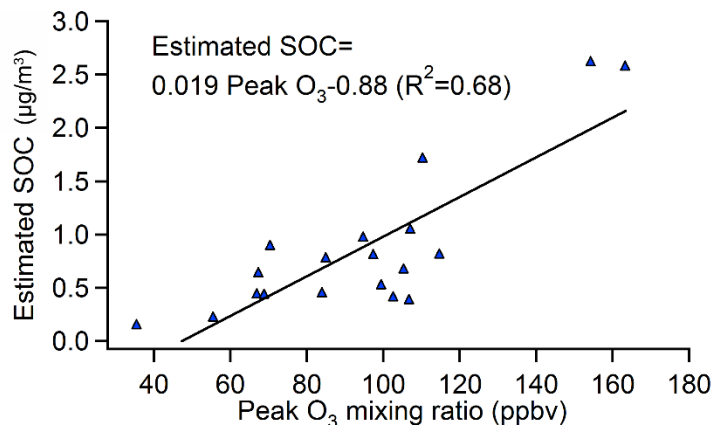
250 Both the EC tracer method and SOA tracer method were used to estimate SOC (details about  
 251 both methods are provided in section S2 of the Supplement). To apply the SOA tracer method,  
 252 the sum of monoterpenes SOA tracers was scaled by a factor of 1.79 (see section S1 and Figure  
 253 S2 for details). Figure S3 compares the SOC estimated by these two methods. SOC estimated by  
 254 EC tracer method ( $SOC_{EC\ tracer}$ ) were generally higher ( $p < 0.01$ ) than those estimated by SOA  
 255 tracer method ( $SOC_{SOA\ tracer}$ ), except for samples TMS1, TMS3 and TMS8. Ding et al. (2012)  
 256 indicated that the EC tracer method might overestimate SOC, because it blended some primary  
 257 OC (POC) from biomass burning with SOC. This inference was supported by the good  
 258 correlation between the difference of SOC estimated by these two methods ( $SOC_{EC\ tracer} - SOC_{SOA\ tracer}$ ) and levoglucosan, a tracer of biomass burning.

260 In addition to levoglucosan, methyl chloride ( $CH_3Cl$ ) is an indicator of biomass burning  
 261 (Rudolph et al., 1995). Figure 3 plots the correlation between levoglucosan and  $CH_3Cl$  at TMS,  
 262 as well as that between  $SOC_{EC\ tracer} - SOC_{SOA\ tracer}$  and levoglucosan. As expected, levoglucosan  
 263 fairly correlated with  $CH_3Cl$  ( $R^2 = 0.54$ ), further confirming the reliability of levoglucosan as the  
 264 tracer of biomass burning. Consistent with Ding et al. (2012), good correlation was found  
 265 between  $SOC_{EC\ tracer} - SOC_{SOA\ tracer}$  and levoglucosan ( $R^2 = 0.52$ ). This verified that the EC tracer  
 266 method overestimated SOC due to the interference of biomass burning. Exceptionally,  $SOC_{EC\ tracer}$   
 267 was remarkably lower than  $SOC_{SOA\ tracer}$  for the samples TMS1, TMS3 and TMS8 ( $p < 0.05$ ).  
 268 Further investigation found that on the sampling days of TMS1 and TMS3, the daily maximum  
 269 hourly  $O_3$  mixing ratio, referred to as peak  $O_3$ , was extremely high, with the values being the

270 second (154.4 ppbv) and first (163.4 ppbv) highest among the 19 filter samples, respectively,  
 271 while during the sampling period of TMS8, the peak O<sub>3</sub> also reached 94.8 ppbv. In contrast, the  
 272 average of peak O<sub>3</sub> values on the sampling days of other PM<sub>2.5</sub> filter samples was only 77.6 ppbv.  
 273 Since high O<sub>3</sub> levels generally imply strong photochemical reactivity, high productions of SOA  
 274 are also expected on these days. Hence, the higher SOC<sub>SOA tracer</sub> values observed in TMS1, TMS3  
 275 and TMS8 were understandable. We also found that there was no correlation between SOC<sub>EC</sub>  
 276 tracer and peak O<sub>3</sub> (not shown), whereas SOC<sub>SOA tracer</sub> correlated well with peak O<sub>3</sub> (R<sup>2</sup>=0.68), as  
 277 shown in Figure 4, implying that the formation of secondary products, *i.e.*, SOA and O<sub>3</sub>, depends  
 278 upon the oxidative capacity of the atmosphere and they may also influence each other. Therefore,  
 279 the SOA tracer method was believed to be more reliable and thus adopted in this study. Hereafter,  
 280 SOC refers to SOC<sub>SOA tracer</sub>, unless otherwise specified.



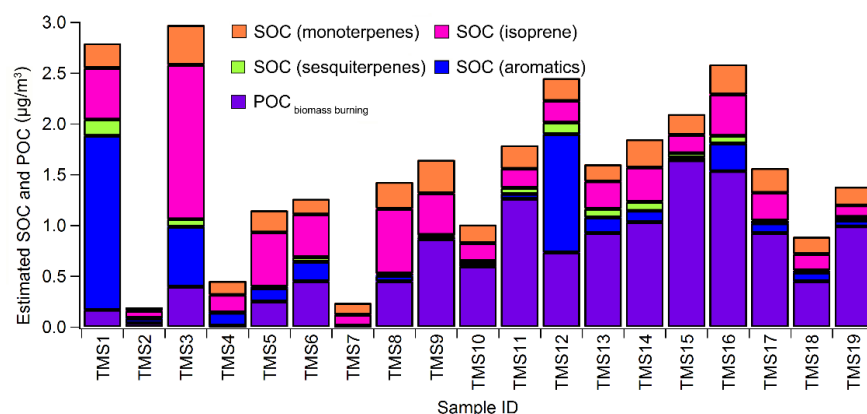
281  
 282 Figure 3 Linear correlations between (a) levoglucosan and CH<sub>3</sub>Cl, and (b) SOC<sub>EC tracer</sub> - SOC<sub>SOA</sub>  
 283 tracer and levoglucosan.



284  
 285 Figure 4 Linear correlation between SOC<sub>SOA tracer</sub> and peak O<sub>3</sub>.

286

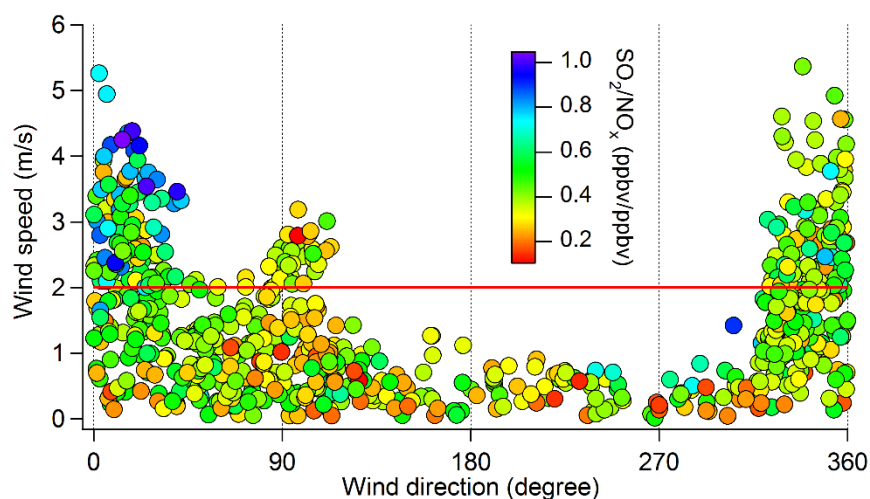
287 Figure 5 shows SOC produced by different groups of VOCs estimated using the SOA tracer  
 288 based approach, and biomass burning related POC ( $\text{POC}_{\text{biomass burning}}$ ).  $\text{POC}_{\text{biomass burning}}$  was  
 289 estimated by  $0.01 (\mu\text{g}/\text{ng}) \times \text{levoglucosan} (\text{ng}/\text{m}^3)$  (Lee et al., 2008). On average, SOC and  $\text{POC}_{\text{biomass burning}}$   
 290 constituted  $0.86 \pm 0.31 \mu\text{g}/\text{m}^3$  ( $17.8 \pm 4.6\%$ ) and  $0.67 \pm 0.22 \mu\text{g}/\text{m}^3$  ( $11.6 \pm 3.2\%$ ) of OC  
 291 (provided in Figure S1), respectively. The rest of OC were undetermined due to unknown  
 292 sources and precursors of OC. The total SOC comprised anthropogenic (*i.e.*, aromatics) and  
 293 biogenic (*i.e.*, isoprene, monoterpenes and sesquiterpenes) SOC, with the fractions of  $21.3 \pm 8.2\%$   
 294 ( $0.26 \pm 0.20 \mu\text{g}/\text{m}^3$ ) and  $78.7 \pm 8.2\%$  ( $0.60 \pm 0.18 \mu\text{g}/\text{m}^3$ ), respectively. Although anthropogenic  
 295 SOC (ASOC) was significantly lower than biogenic SOC (BSOC) ( $p < 0.05$ ), ASOC had its  
 296 highest value of  $1.71 \mu\text{g}/\text{m}^3$  in the sample TMS1, and BSOC reached its maximum in sample  
 297 TMS3 ( $2.03 \mu\text{g}/\text{m}^3$ ). As mentioned earlier, the two samples were collected on the days with very  
 298 high  $\text{O}_3$ , indicating that aromatics and biogenic VOCs might be responsible for the high SOC in  
 299 TMS1 and TMS3, respectively. However, VOC samples were not simultaneously collected  
 300 during the collection of these two samples. Instead, the sample TMS12 was a good example  
 301 because ASOC was the second highest ( $1.2 \mu\text{g}/\text{m}^3$ ), and the daily average mixing ratio of toluene  
 302 coincidentally reached 4.0 ppbv during the TMS12 sampling period, the highest value among all  
 303 VOC samples, which further confirmed the reliability of SOA tracer method in estimating SOC.  
 304 Among SOC derived from biogenic VOCs, isoprene made the highest contribution ( $54.2 \pm 5.3\%$   
 305 of BSOC and  $42.7 \pm 5.9\%$  of total SOC), followed by monoterpenes ( $37.9 \pm 4.6\%$  and  $30.4 \pm 5.5\%$ ,  
 306 respectively) and sesquiterpenes ( $7.9 \pm 2.7\%$  and  $5.6 \pm 1.7\%$ , respectively).



307  
 308 Figure 5 Concentrations of estimated SOC derived from monoterpenes, isoprene, sesquiterpenes  
 309 and aromatics and  $\text{POC}_{\text{biomass burning}}$ .

### 310 3.3 Local and regional contributions to SOC

311 In line with the method used in Guo et al. (2013), the local and regional air masses were  
 312 distinguished with the wind direction (WD) and wind speed (WS) monitored at TMS. Briefly,  
 313 the northerly winds ( $0^\circ < \text{WD} < 90^\circ$  or  $270^\circ < \text{WD} < 360^\circ$ ) with WS higher than 2 m/s were considered  
 314 to be capable of delivering air pollutants from the heavily polluted inland PRD region to the site.  
 315 In these cases, the air masses were believed to be subject to regional influences. Otherwise, the  
 316 site was dominated by local air. To validate this method, Figure 6 shows the hourly ratios of  
 317  $\text{SO}_2/\text{NO}_x$  for the air masses in different wind directions/speeds. Overall, the  $\text{SO}_2/\text{NO}_x$  ratios were  
 318 higher for regional air masses, particularly when  $0^\circ < \text{WD} < 90^\circ$  and  $\text{WS} > 2$  m/s. This coincided  
 319 with the lower sulfur content in vehicle fuels and higher vehicle emissions of  $\text{NO}_x$  in Hong Kong  
 320 (Wang and So, 2003; Guo et al., 2009). For the 24-48 hr  $\text{PM}_{2.5}$  samples (*i.e.*, duration of 1-2  
 321 days), the regional influence was not unexpected given that the northerly wind was stronger than  
 322 2 m/s for at least one hour on each sampling day. It was noteworthy that during the sampling  
 323 periods of TMS1 and TMS16 (influenced by regional air),  $\text{SO}_2$  was exclusively high at the  
 324 HKEPD AQMSs in vicinity of the ship container terminals, *e.g.*, KC, SSP and TW (see Figure 1).  
 325 Figure S4 presents  $\text{SO}_2$  distributions at 14 AQMSs in Hong Kong during these two periods. In  
 326 view of the fact that ship is a significant emitter of  $\text{SO}_2$ , the influence of local ship emission was  
 327 also suspected for the two samples. According to these inferences, Table S2 lists the categories  
 328 of the samples affected by regional air, local air, and local ship emissions, respectively.



329 Figure 6 Hourly ratios of  $\text{SO}_2/\text{NO}_x$  for the air masses in different wind directions/speeds at TMS.  
 330 Table 2 summarizes the concentrations of SOC and  $\text{POC}_{\text{biomass burning}}$  in different categories of air  
 331 masses. Note that since the samples TMS1 and TMS16 were influenced by both regional air and  
 332 local ship emission, they were separately discussed later. It was found that SOC derived from  
 333

334 individual group/species and total SOC in regional air were all significantly ( $p < 0.05$ ) higher than  
 335 that in local air, suggesting that SOC at TMS was elevated by regional transport. Despite  
 336 possible influences of local ship emissions in TMS1 and TMS16, the concentrations of SOC and  
 337 POC in these two samples were well within the ranges of those in regional air, except for  
 338 aromatics SOC ( $1.71 \mu\text{g}/\text{m}^3$ ) in sample TMS1. The extremely high aromatics SOC in TMS1  
 339 might be caused by ship emissions which could be laden with high concentrations of aromatics.  
 340 Contradictorily, SOC derived from aromatics was remarkably lower in TMS16 ( $0.27 \mu\text{g}/\text{m}^3$ ).  
 341 This discrepancy might be explained by the differences of fuel types and operating conditions of  
 342 the ship engines, which were repeatedly proved to affect the emission characteristics of ship  
 343 engines (Reda et al., 2014; Sippula et al., 2014). Similar to SOC, POC also showed a  
 344 significantly higher level in regional air ( $0.81 \pm 0.24 \mu\text{g}/\text{m}^3$ ) than that in local air ( $0.29 \pm 0.35$   
 345  $\mu\text{g}/\text{m}^3$ ) ( $p < 0.05$ ). Since the high concentration of  $\text{POC}_{\text{biomass burning}}$  in regional air was partially  
 346 contributed by TMS16 ( $\text{POC}_{\text{biomass burning}} = 1.54 \mu\text{g}/\text{m}^3$ ), a sample jointly influenced by regional  
 347 air and local ship emission, specific insight was given to this sample. Firstly, ship emission was  
 348 not likely to be the culprit of high  $\text{POC}_{\text{biomass burning}}$ , as no study reported ship emission of  
 349 levoglucosan, the biomass burning tracer used to calculate  $\text{POC}_{\text{biomass burning}}$  in this study. Instead,  
 350 we found that another sample under the influence of regional air (TMS15) had comparable  $\text{POC}_{\text{biomass burning}}$   
 351 ( $1.64 \mu\text{g}/\text{m}^3$ ). Furthermore,  $\text{CH}_3\text{Cl}$ , another tracer of biomass burning, increased  
 352 noticeably under northerly winds in sample TMS16, indicating the regional transport of biomass  
 353 burning plumes into Hong Kong. In fact, nearly no fire spot in local Hong Kong was observed by  
 354 the satellite during the sampling, compared to some open fires detected in upwind directions (see  
 355 Figure S5). Therefore,  $\text{POC}_{\text{biomass burning}}$  in TMS16 was reasonably speculated to be elevated by  
 356 regional biomass burning plumes. Upon this inference, we concluded that regional transport  
 357 significantly contributed to  $\text{PM}_{2.5}$ -bounded POC in Hong Kong.

358

359 Table 2 Mean  $\pm$  95% C.I. of SOC and POC in different categories of air masses (Unit:  $\mu\text{g}/\text{m}^3$ ).

	Local air	Regional air	TMS1 <sup>*</sup>	TMS16 <sup>*</sup>
SOC (monoterpenes)	$0.13 \pm 0.06$	$0.23 \pm 0.03$	0.23	0.28
SOC (isoprene)	$0.16 \pm 0.07$	$0.42 \pm 0.18$	0.51	0.41
SOC (sesquiterpenes)	$0.01 \pm 0.01$	$0.06 \pm 0.02$	0.16	0.07
SOC (aromatics)	$0.07 \pm 0.04$	$0.33 \pm 0.26$	1.71	0.27

POC <sub>biomass burning</sub>	0.29±0.35	0.81±0.24	0.17	1.54
Total SOC	0.37±0.17	1.04±0.39	2.61	1.04

360 \* 95% C.I. is not available for a single sample.

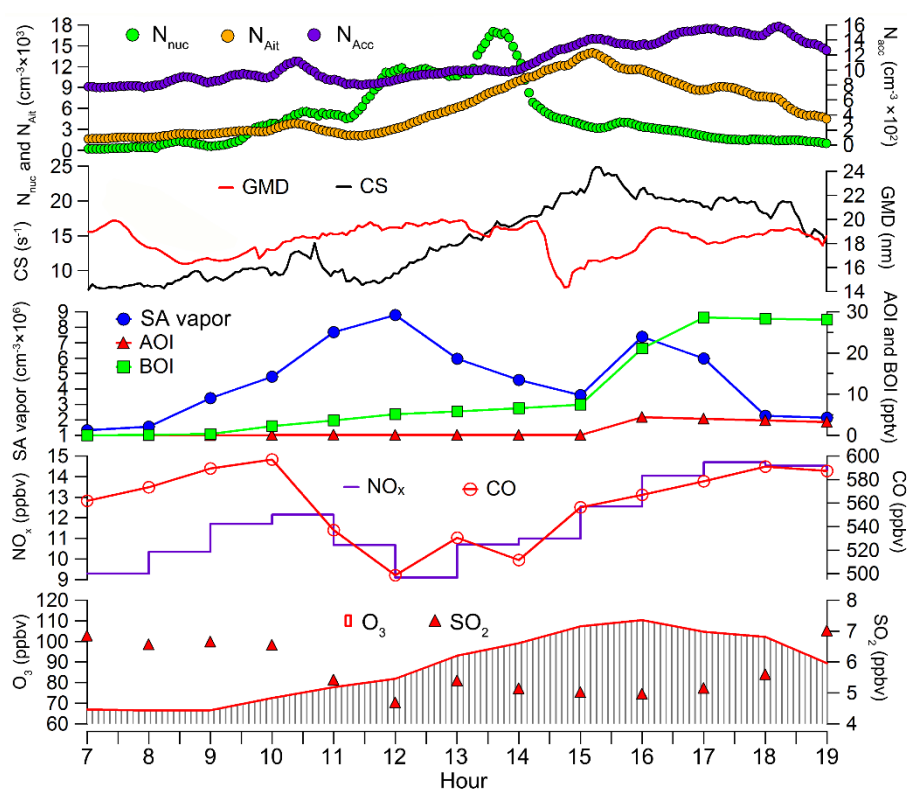
### 361 **3.4 Implications to particle formation and growth**

362 As an important constituent of airborne particles, SOA plays critical role in particle formation  
363 and growth (Jang et al., 2003). The relationships between SOA formation and particle  
364 formation/growth were investigated on three selected days (October 31, November 09 and  
365 November 19) when SOC were among the highest of all the samples and SMPS data were  
366 available. Figures 7-9 show the evolutions of particle numbers, GMD of nucleation mode  
367 particles, CS, the simulated sulfuric acid (SA) vapor, oxidized intermediates of aromatics (AOI),  
368 oxidized intermediates of biogenic VOCs (BOI), and the measured inorganic trace gases. Details  
369 about the modelling of SA vapor, AOI and BOI are provided in Section S3 and Table S3 in the  
370 Supplement. For convenience of analysis, the hourly mixing ratios of biogenic VOCs (BVOCs),  
371 aromatics and CH<sub>3</sub>Cl are presented in Figure S6.

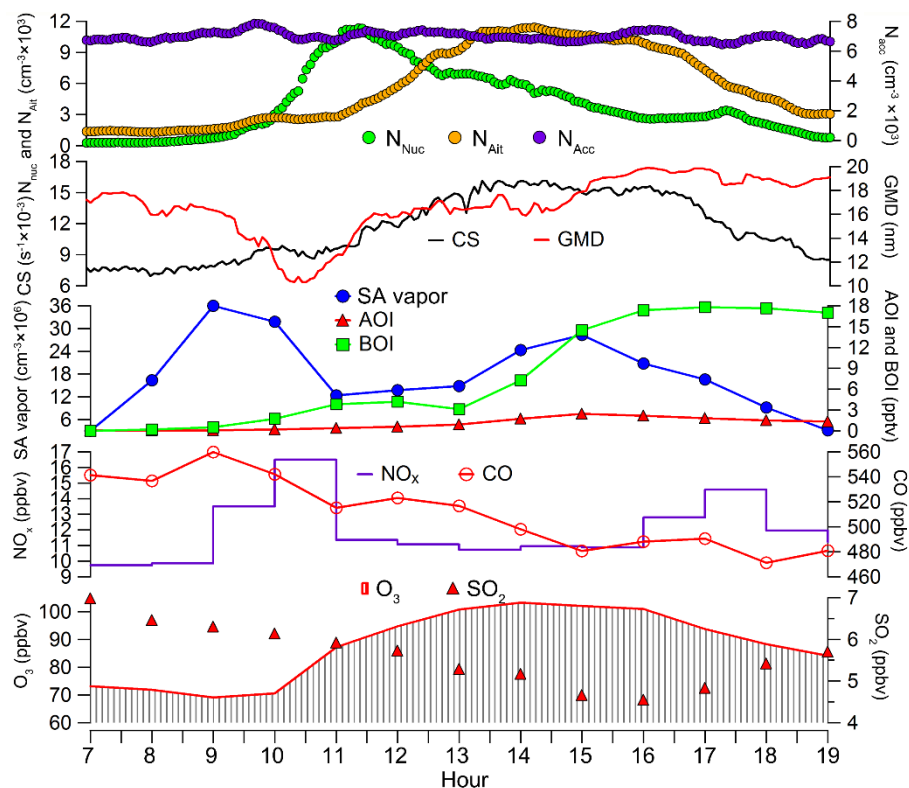
372 In Figures 7-8, the number concentration of nucleation mode particles ( $N_{nuc}$ ) increased  
373 substantially in the morning of October 31 (11:00-12:00) and November 09 (10:00-11:00),  
374 followed by the increases of number of Aitken mode particles ( $N_{Ait}$ ). Prior to the increases of  
375  $N_{nuc}$ , the simulated SA vapor began to increase about 3 hours earlier. These were consistent with  
376 the findings in Guo et al. (2012a) who reported that the increase of  $N_{nuc}$  was caused by new  
377 particle formation (NPF) events occurred on both days, and SA vapor played important roles in  
378 NPF. However, we further found that the oxidation intermediates of BVOCs (*i.e.*, BOI) also  
379 increased slightly ahead of the rise of  $N_{nuc}$ , which might suggest that the oxidation of BVOCs  
380 also made some contributions to NPF. In fact, the involvement of BVOCs in NPF at this  
381 afforested site has been speculated by Guo et al. (2012a), which is confirmed with the aid of  
382 model simulations in this study.

383 Moreover, we noticed that the nucleation mode particles experienced obvious growth with the  
384 rate of 1.9 nm/h (15:00-16:00) and 1.4 nm/h (14:00-16:00) in the afternoon of October 31 and  
385 November 09, respectively. Both growths occurred under the conditions of high  $N_{Ait}$  and high  
386 CS, differing from NPF events. Meanwhile, O<sub>3</sub> was on high level, which meant strong oxidative  
387 capacity of the atmosphere. Correspondingly, the simulated SA vapor, AOI and BOI showed  
388 great increments simultaneously with or 1-2 hours earlier than the increase of GMD. It is

389 noteworthy that the significant increases of AOI and BOI were also attributable to the rapid  
 390 increases of VOCs (see Figure S6), in addition to strong atmospheric oxidative capacity. This  
 391 suggested that the photo-oxidation of VOCs also facilitated the growth of nucleation mode  
 392 particles. The prompt responses of particle growth to the increments of oxidation products on  
 393 October 31 (rather than 1.5 hours' delay on November 09) were likely caused by the much more  
 394 abundant BOI (~22.7 pptv) than that on November 09 (~13.5 pptv). Besides, the lower initial  
 395 GMD before its increase on October 31 (~14 nm compared to ~16 nm on November 09) implied  
 396 higher surface area and subsequently quicker growth. Since the aforementioned days featured  
 397 high SOA, the roles of photo-oxidation of VOCs in the formation and growth of nucleation mode  
 398 particles might reflect the very initial stages of SOA formation. However, to better understand  
 399 the relationships between SOA formation and the formation/growth of particles, data with higher  
 400 resolution and more comprehensive chemical information of SOA are crucially needed.



401  
 402 Figure 7 Evolutions of particle numbers, GMD of nucleation mode particles, CS, simulated SA  
 403 vapor, AOI, BOI and inorganic trace gases on October 31 (first sampling day of TMS12).

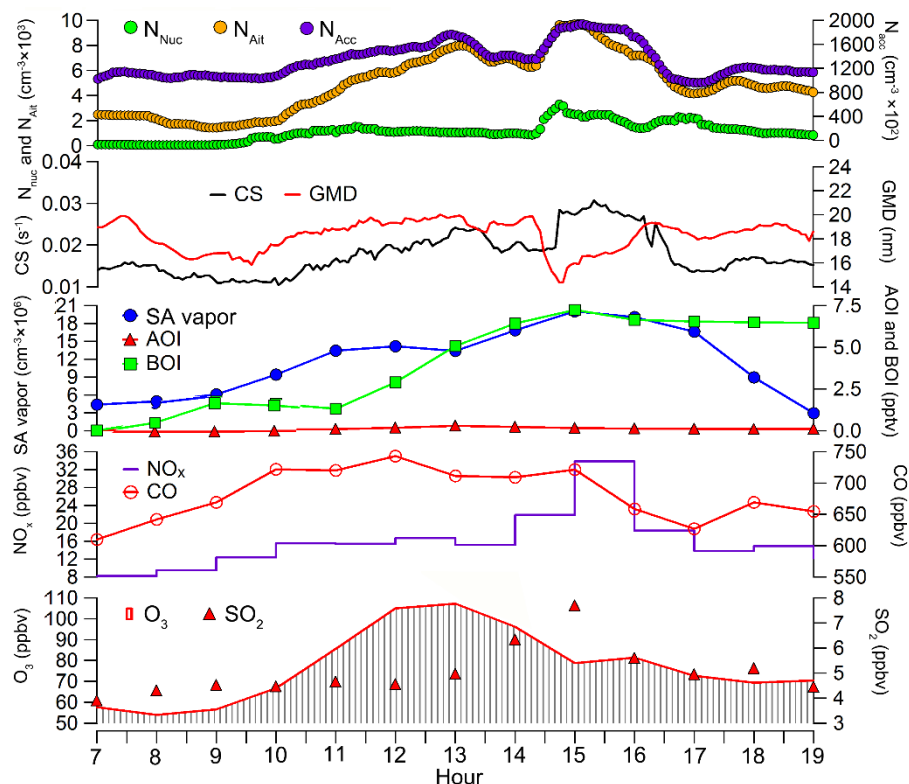


404  
 405 Figure 8 Evolutions of particle numbers, GMD of nucleation mode particles, CS, simulated SA  
 406 vapor, AOI, BOI and inorganic trace gases on November 09 (second sampling day of TMS14).

407  
 408 Similarly, the growth of nucleation mode particles was also observed on November 19 (15:00-  
 409 16:00) (Figure 9). However, a distinct phenomenon was that the numbers of particles in  
 410 nucleation, Aitken and accumulation modes all showed rapid increases simultaneously from  
 411 around 14:30 and reached the highest values at ~15:00, which indicated that the particles in  
 412 different modes shared a common source. Although SO<sub>2</sub> and the simulated SA vapor began to  
 413 increase 1.5 hours earlier, this could not be a NPF event, as the increase of N<sub>Ait</sub> had no delay (no  
 414 banana shape) and the CS was high. In addition, the levels of primary air pollutants (*e.g.*, NO<sub>x</sub>  
 415 and CO) were high at the peak hours of all three-mode particle numbers. More importantly, we  
 416 found that CH<sub>3</sub>Cl largely increased from 13:00 to 15:00 and reached the maximum at 15:00 (see  
 417 Figure S6). Therefore, we suspected that biomass burning might be responsible for the increase  
 418 of particle numbers. This coincided with the high POC<sub>biomass burning</sub> (1.54 μg/m<sup>3</sup>) in PM<sub>2.5</sub> sample  
 419 collected on this day (TMS16). Generally, particles emitted from biomass burning are in Aitken  
 420 and accumulation modes (Reid et al., 2005). However, in vicinity of fire, nucleation mode can  
 421 also exist (Janhall et al., 2010). Here, although nucleation mode particles increased in the particle



422 burst event,  $N_{\text{nuc}}$  was very low (maximum= $2.1 \times 10^3 \text{ cm}^{-3}$ ), indicating that this was not a local  
 423 biomass burning and nucleation mode particles converted to larger size particles from the source  
 424 region to this site. This was also consistent with the regional influence on this day identified by  
 425 the wind fields (see section 3.3).



426 Figure 9 Evolutions of particle numbers, GMD of nucleation mode particles, CS, simulated SA  
 427 vapor, AOI, BOI and inorganic trace gases on November 19 (sampling day of TMS16).  
 428

429

#### 430 4. Conclusions

431  $\text{PM}_{2.5}$  samples were collected at a mountainous site in Hong Kong in autumn of 2010. Nine SOA  
 432 tracers in  $\text{PM}_{2.5}$  were analyzed, which helped to understand the compositions and sources of  
 433 SOC in this study. Results indicated that isoprene made the highest contribution to SOC  
 434 formation at this site, followed by monoterpenes, aromatics and sesquiterpenes. Averagely,  
 435 biogenic SOC dominated over anthropogenic SOC. However, anthropogenic SOC cannot be  
 436 neglected, particularly under the influences of regional transport (e.g.,  $1.2 \mu\text{g}/\text{m}^3$  in sample  
 437 TMS12) and/or local ship emission (e.g.,  $1.7 \mu\text{g}/\text{m}^3$  in sample TMS1). The simultaneous  
 438 observation of VOCs confirmed the role of aromatics in contributing to high concentrations of  
 439 anthropogenic SOC. In terms of SOC origins, regional transport caused nearly two-fold increase

440 of SOC, relative to local air. However, SOC load could also be significantly elevated by local  
441 ship emissions possibly containing abundant VOC precursors and SO<sub>2</sub>, which promoted SOC  
442 formation. In addition, the regional air was generally characterized with high biomass burning  
443 related POC, aggravating the PM<sub>2.5</sub>-bounded POC in Hong Kong. In combination with the SMPS  
444 data, we found that the formation of SOA (particularly the biogenic SOA) might be partially  
445 responsible for the new particle formation and growth of nucleation mode particles. Primary  
446 emissions, such as biomass burning, could cause particle burst events and lead to POC increases.  
447 To our knowledge, this is the first SOA study carried out in low-altitude (640 m) mountainous  
448 area of Hong Kong, where the air quality is under the combined influence of anthropogenic and  
449 biogenic emissions. This study also demonstrates the urgency of data acquisition with more  
450 comprehensive chemical information and higher time resolution in future SOA studies over this  
451 region.

#### 452 **Acknowledgements**

453 This study was supported by the Research Grants Council of the Hong Kong Special  
454 Administrative Region via grants CRF/C5004-15E, PolyU5154/13E, PolyU152052/14E, and  
455 CRF/C5022-14G, and the Hong Kong Polytechnic University PhD scholarships (project #RTUP).  
456 This study is partly supported by the Hong Kong PolyU internal grant (1-BBW4, 4-ZZFW, G-  
457 YBHT and 1-ZVJT) and by the Innovation and Technology Commission of the HKSAR via the  
458 Hong Kong Branch of National Rail Transit Electrification and Automation Engineering  
459 Technology Research Center (1-BBYD).

#### 460 **References**

461 Appel, B.R., Tokiwa, Y., Hsu, J., Kothny, E.L., and Hahn, E., 1985. Visibility as related to  
462 atmospheric aerosol constituents. *Atmos. Environ.* (1967), 19(9), 1525-1534.  
463 Birch, M.E., 1998. Analysis of carbonaceous aerosols: interlaboratory comparison. *Analyst*  
464 123(5), 851-857.  
465 Chameides, W.L., Yu, H., Liu, S.C., Bergin, M., Zhou, X., Mearns, L., Wang, G., Kiang, C.S.,  
466 Saylor, R.D., Luo, C., Huang, Y., Steiner, A., and Giorgi, F., 1999. Case study of the effects of  
467 atmospheric aerosols and regional haze on agriculture: An opportunity to enhance crop yields in  
468 China through emission controls?. *P. Natl. Acad. Sci.* 96(24), 13626-13633.

469 Claeys, M., Graham, B., Vas, G., Wang, W., Vermeylen, R., Pashynska, V., Cafmeyer, J., Guyon,  
470 P., Andreae, M., Artaxo, P., and Maenhaut, W., 2004. Formation of secondary organic aerosols  
471 through photooxidation of isoprene. *Science* 303(5661), 1173-1176.

472 Claeys, M., Szmigielski, R., Kourtchev, I., Van der Veken, P., Vermeylen, R., Maenhaut, W.,  
473 Jaoui, M., Kleindienst, T.E., Lewandowski, M., Offenberg, J.H. and Edney, E.O., 2007.  
474 Hydroxydicarboxylic acids: markers for secondary organic aerosol from the photooxidation of  $\alpha$ -  
475 pinene. *Environ. Sci. Technol.* 41(5), 1628-1634.

476 Ding, X., Wang, X.M., Gao, B., Fu, X.X., He, Q.F., Zhao, X.Y., Yu, J.Z., and Zheng, M., 2012.  
477 Tracer-based estimation of secondary organic carbon in the Pearl River Delta, south China. *J.*  
478 *Geophys. Res.: Atmos.* 117(D5), doi: 10.1029/2011JD016596.

479 Ding, X., Zhang, Y.Q., He, Q.F., Yu, Q.Q., Shen, R.Q., Zhang, Y.L., Zhang, Z., Lyu, S.J., Hu,  
480 Q.H., Wang, Y.S., Li, L.F., Song, W., and Wang, X.M., 2016. Spatial and seasonal variations of  
481 secondary organic aerosol from terpenoids over China. *J. Geophys. Res.: Atmos.* 121, doi:  
482 10.1002/2016JD025467.

483 Dockery, D.W., Pope, C.A., Xu, X., Spengler, J.D., Ware, J.H., Fay, M.E., Ferris Jr., B.G., and  
484 Speizer, F.E., 1993. An association between air pollution and mortality in six US cities. *New*  
485 *Engl. J. Med.* 329(24), 1753-1759.

486 Eddingsaas, N.C., Loza, C.L., Yee, L.D., Chan, M., Schilling, K.A., Chhabra, P.S., Seinfeld J.H.,  
487 and Wennberg, P.O., 2012.  $\alpha$ -pinene photooxidation under controlled chemical conditions-Part 2:  
488 SOA yield and composition in low-and high-NO<sub>x</sub> environments. *Atmos. Chem. Phys.* 12(16),  
489 7413-7427.

490 Forstner, H.J., Flagan, R.C., and Seinfeld, J.H., 1997. Secondary organic aerosol from the  
491 photooxidation of aromatic hydrocarbons: Molecular composition. *Environ. Sci. Technol.* 31(5),  
492 1345-1358.

493 Goldstein, A.H., Koven, C.D., Heald, C.L., and Fung, I.Y., 2009. Biogenic carbon and  
494 anthropogenic pollutants combine to form a cooling haze over the southeastern United States. *P.*  
495 *Natl. Acad. Sci.* 106(22), 8835-8840.

496 Guo, H., Jiang, F., Cheng, H.R., Simpson, I.J., Wang, X.M., Ding, A.J., Wang, T.J., Saunders,  
497 S.M., Wang, T., Lam, S.H.M., Blake, D.R., Zhang, Y.L., and Xie, M., 2009. Concurrent  
498 observations of air pollutants at two sites in the Pearl River Delta and the implication of regional  
499 transport. *Atmos. Chem. Phys.* 9(19), 7343-7360.

500 Guo, H., Lee, S.C., Louie, P.K., Ho, K.F., 2004. Characterization of hydrocarbons, halocarbons  
501 and carbonyls in the atmosphere of Hong Kong. *Chemosphere* 57(10):1363-72.

502 Guo, H., Ling, Z.H., Cheung, K., Jiang, F., Wang, D.W., Simpson, I.J., Barletta, B., Meinardi, S.,  
503 Wang, T.J., Saunders, S.M., and Blake, D.R., 2013. Characterization of photochemical pollution  
504 at different elevations in mountainous areas in Hong Kong. *Atmos. Chem. Phys.* 13(8), 3881-  
505 3898.

506 Guo, H., Ling, Z.H., Simpson, I.J., Blake, D.R., Wang, D.W., 2012b. Observations of isoprene,  
507 methacrolein (MAC) and methyl vinyl ketone (MVK) at a mountain site in Hong Kong. *J.*  
508 *Geophys. Res.: Atmos.* 16;117(D19), doi: 10.1029/2012JD017750.

509 Guo, H., So, K.L., Simpson, I.J., Barletta, B., Meinardi, S., and Blake, D.R., 2007. C<sub>1</sub>-C<sub>8</sub> volatile  
510 organic compounds in the atmosphere of Hong Kong: Overview of atmospheric processing and  
511 source apportionment. *Atmos. Environ.* 41(7), 1456-72.

512 Guo, H., Wang, D.W., Cheung, K., Ling, Z.H., Chan, C.K., and Yao, X.H., 2012a. Observation  
513 of aerosol size distribution and new particle formation at a mountain site in subtropical Hong  
514 Kong. *Atmos. Chem. Phys.* 12(20), 9923-9939.

515 Haddad, I.E., Marchand, N., Temime-Roussel, B., Wortham, H., Piot, C., Besombes, J.L.,  
516 Baduel, C., Voisin, D., Armengaud, A., and Jaffrezo, J.L., 2011. Insights into the secondary  
517 fraction of the organic aerosol in a Mediterranean urban area: Marseille. *Atmos. Chem. Phys.*  
518 11(5), 2059-2079.

519 Huang, J.P., Fung, J.C., and Lau, A.K., 2006. Integrated processes analysis and systematic  
520 meteorological classification of ozone episodes in Hong Kong. *J. Geophys. Res.: Atmos.*  
521 111(D20), doi: 10.1029/2005JD007012.

522 Ho, K.F., Lee, S.C., Guo, H., and Tsai, W.Y., 2004. Seasonal and diurnal variations of volatile  
523 organic compounds (VOCs) in the atmosphere of Hong Kong. *Sci. Total Environ.* 322(1):155-  
524 166.

525 Hu, D., Bian, Q., Li, T.W., Lau, A. K., and Yu, J.Z., 2008. Contributions of isoprene,  
526 monoterpenes,  $\beta$ -caryophyllene, and toluene to secondary organic aerosols in Hong Kong during  
527 the summer of 2006. *J. Geophys. Res.: Atmos.* 113(D22), doi: 10.1029/2008JD010437.

528 Jang, M., Carroll, B., Chandramouli, B., and Kamens, R.M., 2003. Particle growth by acid-  
529 catalyzed heterogeneous reactions of organic carbonyls on preexisting aerosols. *Environ. Sci.*  
530 *Technol.* 37(17), 3828-3837.

531 Jang, M., Czoschke, N.M., Lee, S., and Kamens, R.M., 2002. Heterogeneous atmospheric  
532 aerosol production by acid-catalyzed particle-phase reactions. *Science*, 298(5594), 814-817.

533 Janhall, S., Andreae, M.O., and Poschl, U., 2010. Biomass burning aerosol emissions from  
534 vegetation fires: particle number and mass emission factors and size distributions. *Atmos. chem.*  
535 *Phys.* 10(3), 1427-1439.

536 Kleindienst, T.E., Jaoui, M., Lewandowski, M., Offenberg, J.H., Lewis, C.W., Bhave, P.V., and  
537 Edney, E.O., 2007. Estimates of the contributions of biogenic and anthropogenic hydrocarbons  
538 to secondary organic aerosol at a southeastern US location. *Atmos. Environ.* 41(37), 8288-8300.

539 Kroll, J.H., Ng, N.L., Murphy, S.M., Flagan, R.C., and Seinfeld, J.H., 2006. Secondary organic  
540 aerosol formation from isoprene photooxidation. *Environ. Sci. Technol.* 40(6), 1869-1877.

541 Lee, S., Kim, H.K., Yan, B., Cobb, C.E., Hennigan, C., Nichols, S., Chamber, M., Edgerton, E.S.,  
542 Jansen, J.J., Hu, Y., Zheng, M., Weber, R., and Russell, A.G., 2008. Diagnosis of aged  
543 prescribed burning plumes impacting an urban area. *Environ. Sci. Technol.* 42(5), 1438-1444.

544 Lewandowski, M., Jaoui, M., Offenberg, J.H., Kleindienst, T.E., Edney, E.O., Sheesley, R.J., and  
545 Schauer, J.J. (2008). Primary and secondary contributions to ambient PM in the midwestern  
546 United States. *Environ. Sci. Technol.* 42(9), 3303-3309.

547 Ling, Z.H., Guo, H., Lam, S.H.M., Saunders, S.M., and Wang, T., 2014. Atmospheric  
548 photochemical reactivity and ozone production at two sites in Hong Kong: Application of a  
549 Master Chemical Mechanism–photochemical box model. *J. Geophys. Res.: Atmos.* 119(17),  
550 10567-10582.

551 Maria, S.F., Russell, L.M., Gilles, M.K., and Myneni, S.C., 2004. Organic aerosol growth  
552 mechanisms and their climate-forcing implications. *Science*, 306(5703), 1921-1924.

553 Offenberg, J.H., Lewandowski, M., Jaoui, M., and Kleindienst, T.E., 2011. Contributions of  
554 biogenic and anthropogenic hydrocarbons to secondary organic aerosol during 2006 in Research  
555 Triangle Park, NC. *Aerosol Air Qual. Res.* 11(2), 99-108.

556 Offenberg, J.H., Lewis, C.W., Lewandowski, M., Jaoui, M., Kleindienst, T.E., and Edney, E.O.,  
557 2007. Contributions of toluene and  $\alpha$ -pinene to SOA formed in an irradiated toluene/ $\alpha$ -  
558 pinene/NO<sub>x</sub>/air mixture: Comparison of results using <sup>14</sup>C content and SOA organic tracer  
559 methods. *Environ. Sci. Technol.* 41(11), 3972-3976.

560 Pope III, C.A., and Dockery, D.W., 2006. Health effects of fine particulate air pollution: lines  
561 that connect. *J. Air Waste Manage. Assoc.* 56(6), 709-742.

562 Reda, A.A., Schnelle-Kreis, J., Orasche, J., Abbaszade, G., Lintelmann, J., Arteaga-Salas, J.M.,  
563 Stengel, B., Rade, R., Harndorf, H., Sippula, O., Streibel, T., and Zimmermann, R., 2014. Gas  
564 phase carbonyl compounds in ship emissions: Differences between diesel fuel and heavy fuel oil  
565 operation. *Atmos. Environ.* 94, 467-478.

566 Reid, J.S., Koppmann, R., Eck, T.F., and Eleuterio, D.P., 2005. A review of biomass burning  
567 emissions part II: intensive physical properties of biomass burning particles. *Atmos. Chem. Phys.*  
568 5(3), 799-825.

569 Rudolph, J., Khedim, A., Koppmann, R., and Bonsang, B., 1995. Field study of the emissions of  
570 methyl chloride and other halocarbons from biomass burning in western Africa. *J. Atmos. Chem.*  
571 22(1-2), 67-80.

572 Sippula, O., Stengel, B., Sklorz, M., Streibel, T., Rabe, R., Orasche, J., Lintelmann, J., Michalke,  
573 B., Abbaszade, G., Radischat, C., Groger, T., Schnelle-Kreis, J., Harndorf, H., and Zimmermann,  
574 R., 2014. Particle emissions from a marine engine: chemical composition and aromatic emission  
575 profiles under various operating conditions. *Environ. Sci. Technol.* 48(19), 11721-11729.

576 So, K.L., and Wang, T., 2003. On the local and regional influence on ground-level ozone  
577 concentrations in Hong Kong. *Environ. Pollut.* 123(2), 307-317.

578 Stocker, T.F., Qin, D., Plattner, G.K., et al. IPCC, 2013: climate change 2013: the physical  
579 science basis. Contribution of working group I to the fifth assessment report of the  
580 intergovernmental panel on climate change [J]. 2013.

581 Surratt, J.D., Lewandowski, M., Offenberg, J.H., Jaoui, M., Kleindienst, T.E., Edney, E.O., and  
582 Seinfeld, J.H., 2007. Effect of acidity on secondary organic aerosol formation from isoprene.  
583 *Environ. Sci. Technol.* 41(15), 5363-5369.

584 Volkamer, R., Jimenez, J.L., San Martini, F., Dzepina, K., Zhang, Q., Salcedo, D., Molina, L.T.,  
585 Worsnop, D.R., and Molina, M.J., 2006. Secondary organic aerosol formation from  
586 anthropogenic air pollution: Rapid and higher than expected. *Geophys. Res. Lett.* 33(17), doi:  
587 10.1029/2006GL026899.

588 Williams, B.J., Jayne, J.T., Lambe, A.T., Hohaus, T., Kimmel, J.R., Sueper, D., Brooks, W.,  
589 Williams, L.R., Trimborn, A.M., Martinez, R.E., Hayes, P.L., Jimenez, J.L., Kreisberg, N.M.,  
590 Hering, S.V., Worton, D.R., Goldstein, A.H., and Worsnop, D.R., 2014. The first combined  
591 thermal desorption aerosol gas chromatograph-aerosol mass spectrometer (TAG-AMS). *Aerosol*  
592 *Sci. Technol.* 48(4), 358-370.

**Supplementary material for on-line publication only**

[Click here to download Supplementary material for on-line publication only: Revised supplement material\\_R.docx](#)